Numerical Analysis and Applicable Mathematics

Ariviyal Publishing

Research Article

DOI:10.36686/Ariviyal.NAAM.2020.01.01.002

*Numer. Anal. Appl. Math., 2020, 1(1), 10-26.*

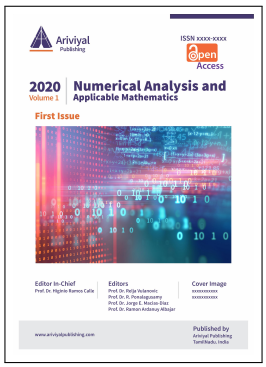


# A Robust HDG Method for Reissner-Mindlin Plate Problems

Gang Chen,[a] Xiaoping Xie*[a] and Yangwen Zhang[b]

[a]*School of Mathematics, Sichuan University, Chengdu 610064, China*
[b]*Department of Mathematical Science, University of Delaware, Newark, DE 19716*

***Corresponding author E-mail address:** *xpxie@scu.edu.cn* (X. Xie)

**ISSN: 2582-8274**

Crossref

**Publication details**
Received 05th May 2020
Revised 13th June 2020
Accepted 15th June 2020
Published 26th June 2020

**Abstract:** We propose and analyze a hybridizable discontinuous Galerkin (HDG) method for Reissner-Mindlin plate problems. The method uses piecewise-polynomials of degree $k(\geq 1)$ to approximate the transverse displacement and the displacement trace on inter-element boundaries, uses piecewise-polynomial vectors of degrees $k$ and $\ell$, $\max(1,k-1)\leq \ell \leq k$, to approximate respectively the rotation and the rotation trace on inter-element boundaries, and uses piecewise-polynomial vectors of degree $k$ and piecewise-polynomial tensors of degree $m$, $k-1\leq m\leq \ell$, to approximate respectively the shear stress and the bending moment. We show that the HDG method is robust in the sense that the derived a priori error estimates are optimal and uniform with respect to the plane thickness $t$. Numerical experiments are performed to confirm our theoretical results.

**Keywords:** Reissner-Mindlin plate; HDG method; error estimate; optimal convergence; uniformly stable

## 1. Introduction

The Reissner–Mindlin (R–M) model describes the deformation of an isotropic homogeneous plate subject to a transverse loading. Due to the avoidance of $C^1$-continuity difficulty, the R-M plate model is a dominating two-dimensional model used to calculate the bending of a thick/thin three-dimensional plate. In this paper we consider the following R-M plate model: find $(\boldsymbol{\theta}, w)$ satisfying

$$\begin{cases} -\nabla\cdot\mathcal{C}\boldsymbol{\epsilon}(\boldsymbol{\theta}) - \lambda t^{-2}(\nabla w-\boldsymbol{\theta}) = \boldsymbol{f}, \ \text{in } \Omega, \\ -\lambda t^{-2}\nabla\cdot(\nabla w-\boldsymbol{\theta}) = g, \ \text{in } \Omega, \end{cases} \tag{1}$$

with the hard clamped (HC) boundary condition

$$\boldsymbol{\theta}=\mathbf{0}, w=0, \ \text{on } \partial\Omega. \tag{2}$$

Here $\Omega\subset\mathbb{R}^2$ is a polygonal domain with boundary $\partial\Omega$, $t$ denotes the plate thickness, $w:\Omega\to\mathbb{R}$ and $\boldsymbol{\theta}:\Omega\to\mathbb{R}^2$ denote the transverse displacement of the midplane and the rotation of the fibers normal to it, which are caused by a body force $\boldsymbol{f}:\Omega\to\mathbb{R}^2$ and the transverse loading $g:\Omega\to\mathbb{R}$. $\boldsymbol{\epsilon}(\cdot)$ is strain operator, i.e. the symmetric part of the gradient which takes values in the space $\mathbb{S}=\mathbb{R}^{2\times 2}_{\rm sym}$ of symmetric $2\times 2$ matrices. The compliance tensor $\mathcal{C}:\mathbb{S}\to\mathbb{S}$ is the module tensor given by

$$\mathcal{C}\boldsymbol{\tau} \quad = \quad \frac{E}{12(1-\nu^2)}\left[(1-\nu)\boldsymbol{\tau}+\nu\mathrm{tr}(\boldsymbol{\tau})I\right], \quad \boldsymbol{\tau}\in\mathbb{S}, \tag{3}$$

and $\lambda=\frac{\kappa E}{2(1+\nu)}$, where $E$ is the Young's modulus, $\nu\in[0,\frac{1}{2})$ the Poisson's ratio, and $\kappa$ the shear correction factor.

It is well-known[1, 7] that low order conforming finite element methods for the Reissner-Mindlin plate model suffer from a performance deterioration, called shear-locking, as the plate thickness $t\to 0$. The locking phenomenon occurs because the requirement $(\nabla w-\boldsymbol{\theta})\to 0$ as $t\to 0$ is too restrictive to allow for good approximations of smooth functions when using low order conforming elements. Therefore, unless the schemes are carefully desired, the locking problems are most likely to happen.

In order to overcome the difficulty of shear-locking, the popular strategy is to introduce a special reduction operator $i_h$ with $(\nabla w-i_h\boldsymbol{\theta})\to 0$ as $t\to 0$ so as to weaken the Kirchhoff constraint; see, e.g.[4, 7, 8, 12, 13, 30, 31, 34, 35, 36, 37, 40, 42, 43, 44, 46, 53] for details. An alternative approach is to employ an equivalent formulation of the original problem, e.g. the formulation using the Helmholtz decomposition,[11] the formulation of displacements and bending moments,[41] and the hybrid stress formulation including variables of displacements, shear stresses and bending moments.[5, 15, 33, 51, 52]

Since the late 1970s, the discontinuous Galerkin (DG) method has become increasingly popular due to its attractive features such as local conservation of physical quantities and flexibility in meshing; see[2, 3] for elliptic boundary value problems. The DG method is also suitable for parallel computation and ideal to be used with $hp$-adaptive strategy. As pointed out in[29], an inconvenient feature of the DG method is that it may require the penalization parameter to be "sufficiently" large (practically unknown) for stability. This inconvenience was avoided by the local discontinuous Galerkin (LDG) method,[28, 16, 14, 25] which has an additional property that fluxes can be eliminated locally. Later, the hybridizable discontinuous Galerkin (HDG) method[23] was devised, which can also overcome this difficulty. The HDG method retains the advantages of the DG method and can significantly reduce the number of degrees of freedom, therefore allowing for a substantial reduction in the computational cost. We refer to[17, 18, 19, 20, 21, 22, 24, 26, 27, 38, 39, 45, 47, 48, 49] for some applications of the HDG method to different PDEs.

In this paper, we propose an arbitrary order HDG scheme to numerically solve the RM plate problems. Thanks to the use of an HDG type mixed form with independent approximations of the transverse displacement, rotation, shear stress and bending moment variables by discontinuous polynomials, the proposed HDG method is shown to be free from shear-locking and to yield optimal convergence rates.

The rest of this paper is organized as follows. Section 2 introduces some basic notations and the HDG scheme for the model problem. Section 3 gives stability results. Section 4 is devoted to the a priori error analysis. Section 5 derives an $L^2$ error estimate for velocity. Finally, Section 8 provides numerical experiments.

Throughout this paper, we use $C$ to denote a positive constant independent of $h$, $h_T$, $h_E$, and $t$, not necessarily the same at each occurrence; we use $a \lesssim b$ to represent $a \leq Cb$.

# 2. The HDG method

## 2.1. Notation

For a bounded domain $\Lambda \subset \mathbb{R}^s$ $(s = 1, 2)$, let $H^m(\Lambda)$ and $H_0^m(\Lambda)$ denote the usual $m^{th}$-order Sobolev spaces on $\Lambda$, and $\|\cdot\|_{m,\Lambda}$, $|\cdot|_{m,\Lambda}$ denote the norm and semi-norm on these spaces. We use $(\cdot,\cdot)_{m,\Lambda}$ to denote the inner product of $H^m(\Lambda)$, with $(\cdot,\cdot)_\Lambda := (\cdot,\cdot)_0, \Lambda$. When $\Lambda = \Omega$, we denote $\|\cdot\|_m := \|\cdot\|_{m,\Omega}, |\cdot|_m := |\cdot|_{m,\Omega}, (\cdot,\cdot) := (\cdot,\cdot)_\Omega$. In particular, when $\Lambda \in \mathbb{R}$, we use $\langle\cdot,\cdot\rangle_\Lambda$ to replace $(\cdot,\cdot)_\Lambda$. We note that bold face fonts will be used for vector (or tensor) analogues of the Sobolev spaces along with vector-valued (or tensor-valued) functions. For an integer $k \geq 0$, $\mathbb{P}_k(\Lambda)$ denotes the set of all polynomials defined on $\Lambda$ with degree at most $k$.

Let $\mathcal{T}_h = \bigcup\{T\}$ be a shape regular triangles partition of the domain $\Omega$. For any $T \in \mathcal{T}_h$, we let $h_T$ be the infimum of the diameters of circles containing $T$ and denote the mesh size $h := \max_{T\in\mathcal{T}_h} h_T$. Let $\mathcal{E}_h = \bigcup\{E\}$ be the union of all edges of $T \in \mathcal{T}_h$. We denote by $h_E$ the length of edge $E$. For all $T \in \mathcal{T}_h$ and $E \in \mathcal{E}_h$, we denote by $\boldsymbol{n}_T$ and $\boldsymbol{n}_E$ the unit outward normal vectors along $\partial T$ and $E$, respectively. We use the mesh-dependent inner products

$$(w, v)_{\mathcal{T}_h} := \sum_{T\in\mathcal{T}_h} (w, v)_T, \qquad \langle\zeta, \rho\rangle_{\partial\mathcal{T}_h} := \sum_{T\in\mathcal{T}_h} \langle\zeta, \rho\rangle_{\partial T},$$

where $(\cdot,\cdot)_D$ denotes the $L^2(D)$ inner product for a set $D \subset \mathbb{R}^2$ and $\langle\cdot,\cdot\rangle_\Gamma$ denotes the $L^2(\Gamma)$ inner product for a set $\Gamma \subset \mathbb{R}^1$. For any finite element functions $w_h$ and $\boldsymbol{r}_h$, let $\nabla w_h$ and $\nabla\cdot\boldsymbol{r}_h$ denote the piecewise gradient and divergence on each element $T \in \mathcal{T}_h$.

## 2.2. Preliminary results

For any element $T \in \mathcal{T}_h$, proper edge $E \in \mathcal{E}_h$ and any nonnegative integer $j$, let $\Pi_j^o : L^2(T) \to \mathbb{P}_j(T)$ and $\Pi_j^\partial : L^2(E) \to \mathbb{P}_j(E)$ be the usual $L^2$ projection operators. Then we can get the following approximation and boundness result.

**Lemma 2.1.** *Let $m$ be an integer with $1 \leq m \leq j+1$. For all $T \in \mathcal{T}_h$, $E \in \mathcal{E}_h$, it holds*

$$\|\Pi_j^o v\|_{0,T} \leq \|v\|_{0,T} \qquad \forall v \in L^2(T), \tag{4a}$$

$$\|\Pi_j^\partial v\|_E \leq \|v\|_E \qquad \forall v \in L^2(E), \tag{4b}$$

$$\|v - \Pi_j^\partial v\|_{\partial T} \lesssim h_T^{m-1/2}|v|_{m,T} \qquad \forall v \in H^m(T), \tag{4c}$$

$$|v - \Pi_j^o v|_{s,T} \lesssim h_T^{m-s}|v|_{m,T} \qquad \forall v \in H^m(T),\ 0 \leq s \leq m, \tag{4d}$$

$$\|\nabla^s(v - \Pi_j^o v)\|_{\partial T} \lesssim h_T^{m-s-1/2}|v|_{m,T} \qquad \forall v \in H^m(T), 1 \leq s+1 \leq m. \tag{4e}$$

Introducing the shear stress vector $\boldsymbol{\gamma} = \lambda t^{-2}(\nabla w - \boldsymbol{\theta})$ and the bending moment tensor $\boldsymbol{\sigma} = \mathcal{C}\boldsymbol{\epsilon}(\boldsymbol{\theta})$, then (1) can be rewriten as:

find $(\boldsymbol{\sigma}, \gamma, \boldsymbol{\theta}, w)$ satisfying

$$\begin{cases} \mathcal{C}^{-1}\boldsymbol{\sigma} - \boldsymbol{\epsilon}(\boldsymbol{\theta}) = 0, \\ -\nabla\cdot\boldsymbol{\sigma} - \gamma = \boldsymbol{f}, \\ -\nabla\cdot\gamma = g, \\ \lambda^{-1}t^2\gamma - (\nabla w - \boldsymbol{\theta}) = 0. \end{cases} \tag{5}$$

A direct calculation shows that

$$\mathcal{C}^{-1}\boldsymbol{\tau} = \frac{12(1+\nu)}{E}\boldsymbol{\tau} - \frac{12\nu}{E}\mathrm{tr}(\boldsymbol{\tau})I$$

and

$$\frac{12(1-\nu)}{E}\|\boldsymbol{\tau}\|_0^2 \le (\mathcal{C}^{-1}\boldsymbol{\tau}, \boldsymbol{\tau}) \le \frac{12(1+\nu)}{E}\|\boldsymbol{\tau}\|_0^2 \tag{6}$$

hold true for any $\boldsymbol{\tau} \in \mathbb{S}$.

To show the regularity of the solution, we introduce the Helmholtz decomposition.

**Lemma 2.2** (c.f [7]). *For $\gamma \in [L^2(\Omega)]^2$, there exists a unique $r \in H_0^1(\Omega)$ and a unique $p \in H^1(\Omega) \cap L_0^2(\Omega)$ such that*

$$\gamma = \nabla r + \nabla^\perp p \quad \text{with } \nabla^\perp p := (\partial p/\partial x_2, -\partial p/\partial x_1)^T. \tag{7}$$

By Lemma 2.2, it is easy to check that problem (5) with boundary condition (2) is equivalent to the following system: find $(r, \boldsymbol{\theta}, \boldsymbol{\sigma}, p, w) \in H^1(\Omega) \times [H_0^1(\Omega)]^2 \times ([L^2(\Omega)]^{2\times 2} \cap \mathbb{S}) \times (H_0^1(\Omega) \cap L_0^2(\Omega)) \times H_0^1(\Omega)$ such that

$$\begin{aligned}
(\nabla r, \nabla\mu) &= (g, \mu), \forall \mu \in H_0^1(\Omega), && \text{(8a)}\\
(\mathcal{C}^{-1}\boldsymbol{\sigma}, \boldsymbol{\tau}) - (\nabla\boldsymbol{\theta}, \boldsymbol{\tau}) &= 0, \forall \boldsymbol{\tau} \in [L^2(\Omega)]^{2\times 2} \cap \mathbb{S}, && \text{(8b)}\\
(\boldsymbol{\sigma}, \nabla\boldsymbol{\phi}) - (\boldsymbol{\phi}, \nabla^\perp p) &= (\nabla r, \boldsymbol{\phi}) + (\boldsymbol{f}, \boldsymbol{\phi}), \forall \boldsymbol{\phi} \in [H_0^1(\Omega)]^2, && \text{(8c)}\\
-(\boldsymbol{\theta}, \nabla^\perp q) - \lambda^{-1}t^2(\nabla^\perp p, \nabla^\perp q) &= 0, q \in H_0^1(\Omega), && \text{(8d)}\\
(\nabla w, \nabla s) &= (\boldsymbol{\theta} + \lambda^{-1}t^2\nabla r, \nabla s), \forall s \in H_0^1(\Omega). && \text{(8e)}
\end{aligned}$$

The following regularity results is found in [7].

**Theorem 2.1.** *Let $\Omega$ be a convex polygon or a smoothly bounded domain. For $\boldsymbol{f} \in [H^{-1}(\Omega)]^2$ and $g \in H^{-1}(\Omega)$, there exists a unique solution $(r, \boldsymbol{\theta}, \boldsymbol{\sigma}, p, w)$ satisfying (8a)-(8e). Moreover, if $\boldsymbol{f} \in [L^2(\Omega)]^2$, then*

$$\|\boldsymbol{\theta}\|_2 + \|\boldsymbol{\sigma}\|_1 + \|r\|_1 + \|p\|_1 + t\|p\|_2 + \|w\|_1 + \|\gamma\|_0 \lesssim \|\boldsymbol{f}\|_0 + \|g\|_{-1}. \tag{9}$$

*In addition, if $g \in L^2(\Omega)$, then*

$$\|r\|_2 + \|w\|_2 + t\|\gamma\|_1 + \|\nabla\cdot\gamma\|_0 \lesssim \|\boldsymbol{f}\|_0 + \|g\|_0. \tag{10}$$

### 2.3. HDG scheme

For any integer $k \ge 1$, $\max(1, k-1) \le \ell \le k$ and $k-1 \le m \le \ell$, we introduce the following finite dimensional spaces:

$$\begin{aligned}
W_h &= \{v_h \in L^2(\Omega) : \ v_h|_T \in \mathbb{P}_k(T), \ \forall T \in \mathcal{T}_h\},\\
\widehat{W}_h &= \{\widehat{v}_h \in L^2(\mathcal{E}_h) : \ \widehat{v}_h|_E \in \mathbb{P}_k(E), \ \forall E \in \mathcal{E}_h\},\\
\widehat{W}_h^0 &= \{\widehat{v}_h \in \widehat{W}_h : \ \widehat{v}_h|_{\partial\Omega} = 0\},\\
\boldsymbol{\Theta}_h &= \{\boldsymbol{\beta}_h \in [L^2(\Omega)]^2 : \ \boldsymbol{\beta}_h|_T \in [\mathbb{P}_k(T)]^2, \ \forall T \in \mathcal{T}_h\},\\
\widehat{\boldsymbol{\Theta}}_h &= \{\widehat{\boldsymbol{\beta}}_h \in [L^2(\mathcal{E}_h)]^2 : \ \widehat{\boldsymbol{\beta}}_h|_E \in [\mathbb{P}_\ell(E)]^2, \ \forall E \in \mathcal{E}_h\},\\
\widehat{\boldsymbol{\Theta}}_h^0 &= \{\widehat{\boldsymbol{\beta}}_h \in \widehat{\boldsymbol{\Theta}}_h : \ \widehat{\boldsymbol{\beta}}_h|_{\partial\Omega} = \mathbf{0}\},\\
\boldsymbol{\Gamma}_h &= \{\boldsymbol{\eta}_h \in [L^2(\Omega)]^2 : \ \boldsymbol{\eta}_h|_T \in [\mathbb{P}_k(T)]^2, \ \forall T \in \mathcal{T}_h\},\\
\boldsymbol{\Sigma}_h &= \{\boldsymbol{\tau}_h \in [L^2(\Omega)]^{2\times 2} : \boldsymbol{\tau}_h^T = \boldsymbol{\tau}_h \text{ and } \boldsymbol{\tau}_h|_T \in [\mathbb{P}_m(T)]^{2\times 2}, \forall T \in \mathcal{T}_h\}.
\end{aligned}$$

Then the HDG formulation in a compact form for the Reissner-Mindlin plate model based on (5) and boundary condition (2) is

given as follows: find $(\boldsymbol{\sigma}_h, \boldsymbol{\gamma}_h, \boldsymbol{\theta}_h, \widehat{\boldsymbol{\theta}}_h, w_h, \widehat{w}_h) \in \boldsymbol{\Sigma}_h \times \boldsymbol{\Gamma}_h \times \boldsymbol{\Theta}_h^0 \times \widehat{\boldsymbol{\Theta}}_h \times W_h \times \widehat{W}_h^0$ such that

$$a_h(\boldsymbol{\sigma}_h, \boldsymbol{\gamma}_h; \boldsymbol{\tau}_h, \boldsymbol{\eta}_h) - b_h(\boldsymbol{\tau}_h, \boldsymbol{\eta}_h; \boldsymbol{\theta}_h, \widehat{\boldsymbol{\theta}}_h, w_h, \widehat{w}_h) = 0, \tag{11a}$$

$$b_h(\boldsymbol{\sigma}_h, \boldsymbol{\gamma}_h; \boldsymbol{\beta}_h, \widehat{\boldsymbol{\beta}}_h, v_h, \widehat{v}_h) + s_h(\boldsymbol{\theta}_h, \widehat{\boldsymbol{\theta}}_h, w_h, \widehat{w}_h; \boldsymbol{\beta}_h, \widehat{\boldsymbol{\beta}}_h, v_h, \widehat{v}_h) = (\boldsymbol{f}, \boldsymbol{\beta}_h) + (g, v_h), \tag{11b}$$

for all $(\boldsymbol{\tau}_h, \boldsymbol{\eta}_h, \boldsymbol{\beta}_h, \widehat{\boldsymbol{\beta}}_h, v_h, \widehat{v}_h) \in \boldsymbol{\Sigma}_h \times \boldsymbol{\Gamma}_h \times \boldsymbol{\Theta}_h \times \widehat{\boldsymbol{\Theta}}_h^0 \times W_h \times \widehat{W}_h^0$, where

$$\begin{aligned}
a_h(\boldsymbol{\sigma}_h, \boldsymbol{\gamma}_h; \boldsymbol{\tau}_h, \boldsymbol{\eta}_h) =& (\mathcal{C}^{-1}\boldsymbol{\sigma}_h, \boldsymbol{\tau}_h)_{\mathcal{T}_h} + \lambda^{-1}t^2(\boldsymbol{\gamma}_h, \boldsymbol{\eta}_h)_{\mathcal{T}_h},\\
b_h(\boldsymbol{\tau}_h, \boldsymbol{\eta}_h; \boldsymbol{\theta}_h, \widehat{\boldsymbol{\theta}}_h, w_h, \widehat{w}_h) =& -(\boldsymbol{\theta}_h, \nabla\cdot\boldsymbol{\tau}_h)_{\mathcal{T}_h} + \langle\widehat{\boldsymbol{\theta}}_h, \boldsymbol{\tau}_h\boldsymbol{n}\rangle_{\partial\mathcal{T}_h} - (w_h, \nabla\cdot\boldsymbol{\eta}_h)_{\mathcal{T}_h} + \langle\widehat{w}_h, \boldsymbol{n}\cdot\boldsymbol{\eta}_h\rangle_{\partial\mathcal{T}_h} - (\boldsymbol{\theta}_h, \boldsymbol{\eta}_h)_{\mathcal{T}_h},\\
s_h(\boldsymbol{\theta}_h, \widehat{\boldsymbol{\theta}}_h, w_h, \widehat{w}_h; \boldsymbol{\beta}_h, \widehat{\boldsymbol{\beta}}_h, v_h, \widehat{v}_h) =& \langle\alpha(\boldsymbol{\Pi}_\ell^\partial\boldsymbol{\theta}_h - \widehat{\boldsymbol{\theta}}_h), \boldsymbol{\Pi}_\ell^\partial\boldsymbol{\beta}_h - \widehat{\boldsymbol{\beta}}_h\rangle_{\partial\mathcal{T}_h} + \langle\alpha(w_h - \widehat{w}_h), v_h - \widehat{v}_h\rangle_{\partial\mathcal{T}_h},
\end{aligned}$$

and the parameter $\alpha$ is taken as

$$\alpha|_E := h_E^{-1} \quad \forall E \in \mathcal{E}_h.$$

**Remark 2.1.** *In fact, one can alternatively choose*

$$\alpha|_{\partial T} := h_T^{-1} \quad \forall T \in \mathcal{T}_h$$

*in the scheme, and this choice makes no difference for the analysis.*

## 3. Stability

We first introduce some basic results.

**Lemma 3.1** (Piecewise Poincaré inequality,[9]). *Under the shape regular condition of $\mathcal{T}_h$, for any $v_p \in H^1(\mathcal{T}_h)$ it holds*

$$\|v_p\|_{\mathcal{T}_h}^2 \lesssim \|\nabla v_p\|_{\mathcal{T}_h}^2 + \sum_{E\in\mathcal{E}_h/\partial\Omega} h_E^{-1}\|\Pi_0^\partial[\![v_p]\!]\|_E^2 + \langle v_p, 1\rangle_{\Gamma_s}^2, \tag{12}$$

*where $\Gamma_s$ is a measurable subset of $\partial\Omega$ with $meas(\Gamma_s) > 0$.*

**Lemma 3.2** (Piecewise Korn's inequality,[10]). *Under the shape regular condition of $\mathcal{T}_h$, for any $\boldsymbol{v}_p \in [H^1(\mathcal{T}_h)]^2$ it holds*

$$\|\nabla\boldsymbol{v}_p\|_{\mathcal{T}_h}^2 \lesssim \|\boldsymbol{\epsilon}(\boldsymbol{v}_p)\|_{\mathcal{T}_h}^2 + \sum_{E\in\mathcal{E}_h/\partial\Omega} h_E^{-1}\|\boldsymbol{\Pi}_1^\partial[\![\boldsymbol{v}_p]\!]\|_E^2 + \sup_{\substack{\boldsymbol{m}\in\mathbb{RM}(\Omega),\\ \|\boldsymbol{m}\|_{\Gamma_s}=1,\\ \int_{\Gamma_s}\boldsymbol{m}\,ds=\boldsymbol{0}}} \langle\boldsymbol{v}_p, \boldsymbol{m}\rangle_{\Gamma_s}^2, \tag{13}$$

*where $\mathbb{RM}(\Omega)$ is the space of (infinitesimal) rigid motions on $\Omega$ defined by*

$$\mathbb{RM}(\Omega) := \left\{\boldsymbol{a} + b\begin{bmatrix} 0 & -1\\ 1 & 0\end{bmatrix}\boldsymbol{x} : \boldsymbol{a}\in\mathbb{R}^2, b\in\mathbb{R}\right\} \tag{14}$$

*for $\boldsymbol{x} \in \Omega$.*

Let us define two semi-norms respectively on $\boldsymbol{\Theta}_h \times \widehat{\boldsymbol{\Theta}}_h^0$ and $W_h \times \widehat{W}_h^0$:

$$\begin{aligned}
\|(\boldsymbol{\theta}_h, \widehat{\boldsymbol{\theta}}_h)\|_\Theta^2 :=& \|\boldsymbol{\epsilon}(\boldsymbol{\theta}_h)\|_{\mathcal{T}_h}^2 + \|\alpha^{1/2}(\boldsymbol{\Pi}_\ell^\partial\boldsymbol{\theta}_h - \widehat{\boldsymbol{\theta}}_h)\|_{\partial\mathcal{T}_h}^2, \quad \forall(\boldsymbol{\theta}_h, \widehat{\boldsymbol{\theta}}_h) \in \boldsymbol{\Theta}_h \times \widehat{\boldsymbol{\Theta}}_h^0,\\
\|(w_h, \widehat{w}_h)\|_W^2 :=& \|\nabla w_h\|_{\mathcal{T}_h}^2 + \|\alpha^{1/2}(w_h - \widehat{w}_h)\|_{\partial\mathcal{T}_h}^2, \quad \forall(w_h, \widehat{w}_h) \in W_h \times \widehat{W}_h^0.
\end{aligned}$$

By Lemmas 3.1-3.2, we can prove the following HDG-Poincaré and HDG-Korn's inequalities.

**Lemma 3.3.** *For any $(\boldsymbol{\theta}_h, \widehat{\boldsymbol{\theta}}_h) \in \boldsymbol{\Theta}_h \times \widehat{\boldsymbol{\Theta}}_h^0$ and sufficiently small $h$, it holds*

$$\|\boldsymbol{\theta}_h\|_{\mathcal{T}_h} + \|\nabla\boldsymbol{\theta}_h\|_{\mathcal{T}_h} \lesssim \|(\boldsymbol{\theta}_h, \widehat{\boldsymbol{\theta}}_h)\|_\Theta. \tag{15}$$

*Proof.* For $(\boldsymbol{\theta}_h, \widehat{\boldsymbol{\theta}}_h) \in \boldsymbol{\Theta}_h \times \widehat{\boldsymbol{\Theta}}_h^0$ we apply Lemma 3.2, Cauchy-Schwarz inequality and $\max(1, k-1) \le \ell \le k$ to get

$$\begin{aligned}
\|\nabla \boldsymbol{\theta}_h\|_{\mathcal{T}_h}^2 &\lesssim \|\boldsymbol{\epsilon}(\boldsymbol{\theta}_h)\|_{\mathcal{T}_h}^2 + \sum_{E\in\mathcal{E}_h/\partial\Omega} h_E^{-1}\|\boldsymbol{\Pi}_1^\partial[\![\boldsymbol{\theta}_h]\!]\|_E^2 + \|\boldsymbol{\theta}_h\|_{\partial\Omega}^2 \\
&\le \|\boldsymbol{\epsilon}(\boldsymbol{\theta}_h)\|_{\mathcal{T}_h}^2 + \sum_{E\in\mathcal{E}_h/\partial\Omega} h_E^{-1}\|\boldsymbol{\Pi}_\ell^\partial[\![\boldsymbol{\theta}_h]\!]\|_E^2 + \|\boldsymbol{\theta}_h\|_{\partial\Omega}^2 \\
&= \|\boldsymbol{\epsilon}(\boldsymbol{\theta}_h)\|_{\mathcal{T}_h}^2 + \sum_{E\in\mathcal{E}_h/\partial\Omega} h_E^{-1}\|[\![\boldsymbol{\Pi}_\ell^\partial\boldsymbol{\theta}_h - \widehat{\boldsymbol{\theta}}_h]\!]\|_E^2 + \|\boldsymbol{\theta}_h - \widehat{\boldsymbol{\theta}}_h\|_{\partial\Omega}^2 \\
&\lesssim \|\boldsymbol{\epsilon}(\boldsymbol{\theta}_h)\|_{\mathcal{T}_h}^2 + \sum_{E\in\mathcal{E}_h/\partial\Omega} h_E^{-1}\|[\![\boldsymbol{\Pi}_\ell^\partial\boldsymbol{\theta}_h - \widehat{\boldsymbol{\theta}}_h]\!]\|_E^2 + \|\boldsymbol{\Pi}_\ell^\partial\boldsymbol{\theta}_h - \widehat{\boldsymbol{\theta}}_h\|_{\partial\Omega}^2 + \|\boldsymbol{\theta}_h - \boldsymbol{\Pi}_\ell^\partial\boldsymbol{\theta}_h\|_{\partial\Omega}^2 \\
&\lesssim \|\boldsymbol{\epsilon}(\boldsymbol{\theta}_h)\|_{\mathcal{T}_h}^2 + \sum_{T\in\mathcal{T}_h} h_T^{-1}\|\boldsymbol{\Pi}_\ell^\partial\boldsymbol{\theta}_h - \widehat{\boldsymbol{\theta}}_h\|_{\partial T}^2 + h\|\nabla\boldsymbol{\theta}_h\|_{\mathcal{T}_h}^2.
\end{aligned}$$

Then for sufficiently small $h$ it holds

$$\|\nabla\boldsymbol{\theta}_h\|_{\mathcal{T}_h} \lesssim \|(\boldsymbol{\theta}_h, \widehat{\boldsymbol{\theta}}_h)\|_\Theta.$$

Similarly, by the triangle inequality, Lemma 3.1 and (15), we have

$$\|\boldsymbol{\theta}_h\|_{\mathcal{T}_h}^2 \lesssim \|\nabla\boldsymbol{\theta}_h\|_{\mathcal{T}_h}^2 + \sum_{E\in\mathcal{E}_h/\partial\Omega} h_E^{-1}\|\boldsymbol{\Pi}_0^\partial[\![\boldsymbol{\theta}_h]\!]\|_E^2 + \|\boldsymbol{\theta}_h\|_{\partial\Omega}^2 \lesssim \|(\boldsymbol{\theta}_h, \widehat{\boldsymbol{\theta}}_h)\|_\Theta^2.$$

As a result, the desired estimate (15) follows. □

Using Lemma 3.3, we easily obtain the following inf-sup stability condition.

**Theorem 3.1.** *For all $(\boldsymbol{\theta}_h, \widehat{\boldsymbol{\theta}}_h, w_h, \widehat{w}_h) \in \boldsymbol{\Theta}_h \times \widehat{\boldsymbol{\Theta}}_h^0 \times W_h \times \widehat{W}_h^0$, it holds*

$$\|(\boldsymbol{\theta}_h, \widehat{\boldsymbol{\theta}}_h)\|_\Theta + \|(w_h, \widehat{w}_h)\|_W \lesssim \sup_{\mathbf{0}\neq(\boldsymbol{\tau}_h,\boldsymbol{\eta}_h)\in\boldsymbol{\Sigma}_h\times\boldsymbol{\Gamma}_h} \frac{b_h(\boldsymbol{\tau}_h, \boldsymbol{\eta}_h; \boldsymbol{\theta}_h, \widehat{\boldsymbol{\theta}}_h, w_h, \widehat{w}_h)}{\|\boldsymbol{\tau}_h\|_0 + t\|\boldsymbol{\eta}_h\|_0} + s_h(\boldsymbol{\theta}_h, \widehat{\boldsymbol{\theta}}_h, w_h, \widehat{w}_h; \boldsymbol{\theta}_h, \widehat{\boldsymbol{\theta}}_h, w_h, \widehat{w}_h)^{1/2}.$$

*Proof.* To simplify the notation, we introduce the following two positive constants:

$$C_{\inf} := \frac{12(1-\nu)}{E}, \quad C_P := \sup_{\mathbf{0}\neq(\boldsymbol{\beta},\widehat{\boldsymbol{\beta}}_h)\in\boldsymbol{\Theta}_h\times\widehat{\boldsymbol{\Theta}}_h^0} \frac{\|\boldsymbol{\beta}_h\|_{\mathcal{T}_h}}{\|(\boldsymbol{\beta}_h, \widehat{\boldsymbol{\beta}}_h)\|_\Theta}. \tag{16}$$

Notice that $C_P$ is independent of $t$ and $h$ due to (15). Let $C_0$ be a constant to be defined later. For $(\boldsymbol{\theta}_h, w_h) \in \boldsymbol{\Theta}_h \times W_h$, we take $\boldsymbol{\tau}_h \in \boldsymbol{\Sigma}_h$, with $\boldsymbol{\tau}_h|_T = \boldsymbol{\epsilon}(\boldsymbol{\theta}_h|_T)$ for any $T \in \mathcal{T}_h$, and $\boldsymbol{\eta}_h = C_0(\nabla w_h + \boldsymbol{\theta}_h) \in \boldsymbol{\Gamma}_h$, and use (6) and (16) to get

$$\begin{aligned}
&b_h(\boldsymbol{\tau}_h, \boldsymbol{\eta}_h; \boldsymbol{\theta}_h, \widehat{\boldsymbol{\theta}}_h, w_h, \widehat{w}_h) \\
&\quad= \|\boldsymbol{\epsilon}(\boldsymbol{\theta}_h)\|_{\mathcal{T}_h}^2 + C_0\|\nabla w_h\|_{\mathcal{T}_h}^2 - C_0\|\boldsymbol{\theta}_h\|_{\mathcal{T}_h}^2 + \langle\widehat{\boldsymbol{\theta}}_h - \boldsymbol{\Pi}_\ell^\partial\boldsymbol{\theta}_h, \boldsymbol{\epsilon}_h(\boldsymbol{\theta}_h)\boldsymbol{n}\rangle_{\partial\mathcal{T}_h} + \langle\widehat{w}_h - w_h, \boldsymbol{n}\cdot C_0(\nabla w_h + \boldsymbol{\theta}_h)\rangle_{\partial\mathcal{T}_h} \\
&\quad\ge \frac{1}{2}\|(\boldsymbol{\theta}_h, \widehat{\boldsymbol{\theta}}_h)\|_\Theta^2 + \frac{C_0}{2}\|(w_h, \widehat{w}_h)\|_W^2 - C_P^2C_0\|(\boldsymbol{\theta}_h, \widehat{\boldsymbol{\theta}}_h)\|_\Theta^2 - C_1 s_h(\boldsymbol{\theta}_h, \widehat{\boldsymbol{\theta}}_h, w_h, \widehat{w}_h; \boldsymbol{\theta}_h, \widehat{\boldsymbol{\theta}}_h, w_h, \widehat{w}_h) \\
&\quad\ge \left(\frac{1}{2} - C_P^2C_0\right)\|(\boldsymbol{\theta}_h, \widehat{\boldsymbol{\theta}}_h)\|_\Theta^2 + \frac{C_0}{2}\|(w_h, \widehat{w}_h)\|_W^2 - C_1 s_h(\boldsymbol{\theta}_h, \widehat{\boldsymbol{\theta}}_h, w_h, \widehat{w}_h; \boldsymbol{\theta}_h, \widehat{\boldsymbol{\theta}}_h, w_h, \widehat{w}_h)^{1/2}\left(\|\boldsymbol{\theta}_h, \widehat{\boldsymbol{\theta}}_h\|_\Theta + \|(w_h, \widehat{w}_h)\|_W\right),
\end{aligned}$$

and

$$\|\boldsymbol{\tau}_h\|_{\mathcal{T}_h} + t\|\boldsymbol{\eta}_h\|_{\mathcal{T}_h} \le \max(1 + tC_PC_0, tC_0)(\|(\boldsymbol{\theta}_h, \widehat{\boldsymbol{\theta}}_h)\|_\Theta + \|(w_h, \widehat{w}_h)\|_W).$$

Combine the two inequalities above and take $C_0 = C_P^{-2}/4$, this gives

$$\begin{aligned}
\sup_{\mathbf{0}\neq(\boldsymbol{\tau}_h,\boldsymbol{\eta}_h)\in\boldsymbol{\Sigma}_h\times\boldsymbol{\Gamma}_h} \frac{b_h(\boldsymbol{\tau}_h, \boldsymbol{\eta}_h; \boldsymbol{\theta}_h, \widehat{\boldsymbol{\theta}}_h, w_h, \widehat{w}_h)}{\|\boldsymbol{\tau}_h\|_{\mathcal{T}_h} + \|\boldsymbol{\eta}_h\|_{\mathcal{T}_h}} &\ge \frac{\min(1, C_P^{-2})}{16\max(1 + tC_PC_0, tC_0)}(\|(\boldsymbol{\theta}_h, \widehat{\boldsymbol{\theta}}_h)\|_\Theta + \|(w_h, \widehat{w}_h)\|_W) \\
&\quad - \frac{C_1}{\max(1 + tC_PC_0, tC_0)} s_h(\boldsymbol{\theta}_h, \widehat{\boldsymbol{\theta}}_h, w_h, \widehat{w}_h; \boldsymbol{\theta}_h, \widehat{\boldsymbol{\theta}}_h, w_h, \widehat{w}_h)^{1/2}.
\end{aligned}$$

This yields the desired conclusion. □

# 4. A Priori Error Estimates

## 4.1. Primary error estimates

**Lemma 4.1.** *Let $(\boldsymbol{\sigma},\boldsymbol{\gamma},\boldsymbol{\theta},w)\in([L^2(\Omega)]^{2\times 2}\cap\mathbb{S})\times[L^2(\Omega)]^2\times[H_0^1(\Omega)]^2\times H_0^1(\Omega)$ be the weak solution to problem (5) with boundary condition (2), then, for all $(\boldsymbol{\tau}_h,\boldsymbol{\eta}_h,\boldsymbol{\beta}_h,\widehat{\boldsymbol{\beta}}_h,v_h,\widehat{v}_h)\in\boldsymbol{\Sigma}_h\times\boldsymbol{\Gamma}_h\times\boldsymbol{\Theta}_h\times\widehat{\boldsymbol{\Theta}}_h^0\times W_h\times\widehat{W}_h^0$, it holds*

$$a_h(\boldsymbol{\Pi}_m^o\boldsymbol{\sigma},\boldsymbol{\Pi}_k^o\boldsymbol{\gamma};\boldsymbol{\tau}_h,\boldsymbol{\eta}_h)-b_h(\boldsymbol{\tau}_h,\boldsymbol{\eta}_h;\boldsymbol{\Pi}_k^o\boldsymbol{\theta},\boldsymbol{\Pi}_\ell^\partial\boldsymbol{\theta},\Pi_k^o w,\Pi_k^\partial w)=0, \tag{17a}$$

$$b_h(\boldsymbol{\Pi}_m^o\boldsymbol{\sigma},\boldsymbol{\Pi}_k^o\boldsymbol{\gamma};\boldsymbol{\beta}_h,\widehat{\boldsymbol{\beta}}_h,v_h,\widehat{v}_h)+s_h(\boldsymbol{\Pi}_k^o\boldsymbol{\theta},\boldsymbol{\Pi}_\ell^\partial\boldsymbol{\theta},\Pi_k^o w,\Pi_k^\partial w;\boldsymbol{\beta}_h,\widehat{\boldsymbol{\beta}}_h,v_h,\widehat{v}_h)=(\boldsymbol{f},\boldsymbol{\beta}_h)+(g,v_h)+E(\boldsymbol{\beta}_h,\widehat{\boldsymbol{\beta}}_h,v_h,\widehat{v}_h), \tag{17b}$$

*where*

$$\begin{aligned}E(\boldsymbol{\beta}_h,\widehat{\boldsymbol{\beta}}_h,v_h,\widehat{v}_h)=&s_h(\boldsymbol{\Pi}_k^o\boldsymbol{\theta},\boldsymbol{\Pi}_\ell^\partial\boldsymbol{\theta},\Pi_k^o w,\Pi_k^\partial w;\boldsymbol{\beta}_h,\widehat{\boldsymbol{\beta}}_h,v_h,\widehat{v}_h)-(v_h,\nabla\cdot\boldsymbol{\Pi}_k^o\nabla^\perp p)_{\mathcal{T}_h}+\langle\widehat{v}_h,\boldsymbol{n}\cdot\boldsymbol{\Pi}_k^o\nabla^\perp p\rangle_{\partial\mathcal{T}_h}\\&+\langle\widehat{\boldsymbol{\beta}}_h-\boldsymbol{\beta}_h,\boldsymbol{\Pi}_m^o\boldsymbol{\sigma}\boldsymbol{n}-\boldsymbol{\sigma}\boldsymbol{n}\rangle_{\partial\mathcal{T}_h}+\langle\widehat{v}_h-v_h,\boldsymbol{\Pi}_k^o\nabla r\cdot\boldsymbol{n}-\nabla r\cdot\boldsymbol{n}\rangle_{\partial\mathcal{T}_h}.\end{aligned}$$

*Proof.* By the definitions of $a_h$ and $b_h$, we get

$$\begin{aligned}&a_h(\boldsymbol{\Pi}_m^o\boldsymbol{\sigma},\boldsymbol{\Pi}_k^o\boldsymbol{\gamma};\boldsymbol{\tau}_h,\boldsymbol{\eta}_h)-b_h(\boldsymbol{\tau}_h,\boldsymbol{\eta}_h;\boldsymbol{\Pi}_k^o\boldsymbol{\theta},\boldsymbol{\Pi}_\ell^\partial\boldsymbol{\theta},\Pi_k^o w,\Pi_k^\partial w)\\=&(\mathcal{C}^{-1}\boldsymbol{\Pi}_k^o\boldsymbol{\sigma},\boldsymbol{\tau}_h)_{\mathcal{T}_h}+\lambda^{-1}t^2(\boldsymbol{\Pi}_k^o\boldsymbol{\gamma},\boldsymbol{\eta}_h)_{\mathcal{T}_h}+(\boldsymbol{\Pi}_k^o\boldsymbol{\theta},\nabla\cdot\boldsymbol{\tau}_h)_{\mathcal{T}_h}-\langle\boldsymbol{\Pi}_\ell^\partial\boldsymbol{\theta},\boldsymbol{\tau}_h\boldsymbol{n}\rangle_{\partial\mathcal{T}_h}\\&+(\Pi_k^o w,\nabla\cdot\boldsymbol{\eta}_h)_{\mathcal{T}_h}-\langle\Pi_k^\partial w,\nabla\cdot\boldsymbol{\eta}_h\rangle_{\partial\mathcal{T}_h}+(\boldsymbol{\Pi}_k^o\boldsymbol{\theta},\boldsymbol{\eta}_h)_{\mathcal{T}_h}.\end{aligned}$$

Apply the orthogonality of $L^2$ projection, integration by parts and (5) to get

$$a_h(\boldsymbol{\Pi}_m^o\boldsymbol{\sigma},\boldsymbol{\Pi}_k^o\boldsymbol{\gamma};\boldsymbol{\tau}_h,\boldsymbol{\eta}_h)-b_h(\boldsymbol{\tau}_h,\boldsymbol{\eta}_h;\boldsymbol{\Pi}_k^o\boldsymbol{\theta},\boldsymbol{\Pi}_\ell^\partial\boldsymbol{\theta},\Pi_k^o w,\Pi_k^\partial w)=(\mathcal{C}^{-1}\boldsymbol{\sigma}-\boldsymbol{\epsilon}(\boldsymbol{\theta}),\boldsymbol{\tau}_h)_{\mathcal{T}_h}+(\lambda^{-1}t^2\boldsymbol{\gamma}-\nabla w+\boldsymbol{\theta},\boldsymbol{\eta}_h)_{\mathcal{T}_h}=0$$

and

$$\begin{aligned}b_h(\boldsymbol{\Pi}_m^o\boldsymbol{\sigma},\boldsymbol{\Pi}_k^o\boldsymbol{\gamma};\boldsymbol{\beta}_h,\widehat{\boldsymbol{\beta}}_h,v_h,\widehat{v}_h)=&-(\boldsymbol{\beta}_h,\nabla\cdot\boldsymbol{\Pi}_m^o\boldsymbol{\sigma})_{\mathcal{T}_h}+\langle\widehat{\boldsymbol{\beta}}_h,\boldsymbol{\Pi}_m^o\boldsymbol{\sigma}\cdot\boldsymbol{n}\rangle_{\partial\mathcal{T}_h}-(v_h,\nabla\cdot\boldsymbol{\Pi}_k^o\nabla r)_{\mathcal{T}_h}\\&+\langle\widehat{v}_h,\boldsymbol{n}\cdot\boldsymbol{\Pi}_k^o\nabla r\rangle_{\partial\mathcal{T}_h}-(v_h,\nabla\cdot\boldsymbol{\Pi}_k^o\nabla^\perp p)_{\mathcal{T}_h}+\langle\widehat{v}_h,\boldsymbol{n}\cdot\boldsymbol{\Pi}_k^o\nabla^\perp p\rangle_{\partial\mathcal{T}_h}-(\boldsymbol{\beta}_h,\boldsymbol{\Pi}_k^o\boldsymbol{\gamma})_{\mathcal{T}_h}\\=&-(\boldsymbol{\beta}_h,\nabla\cdot\boldsymbol{\sigma})_{\mathcal{T}_h}+\langle\widehat{\boldsymbol{\beta}}_h-\boldsymbol{\beta}_h,(\boldsymbol{\Pi}_m^o\boldsymbol{\sigma}-\boldsymbol{\sigma})\cdot\boldsymbol{n}\rangle_{\partial\mathcal{T}_h}-(v_h,\Delta r)_{\mathcal{T}_h}\\&+\langle\widehat{v}_h-v_h,\boldsymbol{n}\cdot(\boldsymbol{\Pi}_k^o\nabla r-\nabla r)\rangle_{\partial\mathcal{T}_h}-(v_h,\nabla\cdot\boldsymbol{\Pi}_k^o\nabla^\perp p)_{\mathcal{T}_h}+\langle\widehat{v}_h,\boldsymbol{n}\cdot\boldsymbol{\Pi}_k^o\nabla^\perp p\rangle_{\partial\mathcal{T}_h}-(\boldsymbol{\beta}_h,\boldsymbol{\gamma})_{\mathcal{T}_h}\\=&(\boldsymbol{f},\boldsymbol{\beta}_h)_{\mathcal{T}_h}+(g,v_h)_{\mathcal{T}_h}+\langle\widehat{\boldsymbol{\beta}}_h-\boldsymbol{\beta}_h,\boldsymbol{\Pi}_m^o\boldsymbol{\sigma}\boldsymbol{n}-\boldsymbol{\sigma}\boldsymbol{n}\rangle_{\partial\mathcal{T}_h}+\langle\widehat{v}_h-v_h,\boldsymbol{\Pi}_k^o\nabla r\cdot\boldsymbol{n}-\nabla r\cdot\boldsymbol{n}\rangle_{\partial\mathcal{T}_h}\\&-(v_h,\nabla\cdot\boldsymbol{\Pi}_k^o\nabla^\perp p)_{\mathcal{T}_h}+\langle\widehat{v}_h,\boldsymbol{n}\cdot\boldsymbol{\Pi}_k^o\nabla^\perp p\rangle_{\partial\mathcal{T}_h},\end{aligned}$$

where we have used the relations $\langle\widehat{\boldsymbol{\beta}}_h,\boldsymbol{\sigma}\boldsymbol{n}\rangle_{\partial\mathcal{T}_h}=0$, $\langle\widehat{v}_h,\nabla r\cdot\boldsymbol{n}\rangle_{\partial\mathcal{T}_h}=0$, $\nabla\cdot\boldsymbol{\sigma}=\boldsymbol{f}$ and $-\Delta r=g$. Thus, the desired relations (17a)-(17b) follow. □

To simplify the notations, we set

$$\begin{aligned}\boldsymbol{\xi}_h^\sigma&:=\boldsymbol{\Pi}_m^o\boldsymbol{\sigma}-\boldsymbol{\sigma}_h,\quad\boldsymbol{\xi}_h^\gamma:=\boldsymbol{\Pi}_k^o\boldsymbol{\gamma}-\boldsymbol{\gamma}_h,\\\boldsymbol{\xi}_h^\theta&:=\boldsymbol{\Pi}_k^o\boldsymbol{\theta}-\boldsymbol{\theta}_h,\quad\xi_h^w:=\Pi_k^o w-w_h,\\\boldsymbol{\xi}_h^{\widehat{\theta}}&:=\boldsymbol{\Pi}_\ell^\partial\boldsymbol{\theta}-\widehat{\boldsymbol{\theta}}_h,\quad\xi_h^{\widehat{w}}:=\Pi_k^\partial w-\widehat{w}_h.\end{aligned}$$

**Lemma 4.2.** *For any $\boldsymbol{\eta}_h\in\boldsymbol{\Gamma}_h$, it holds*

$$-(\xi_h^w,\nabla\cdot\boldsymbol{\eta}_h)_{\mathcal{T}_h}+\langle\xi_h^{\widehat{w}},\nabla\cdot\boldsymbol{\eta}_h\rangle_{\partial\mathcal{T}_h}=(\boldsymbol{\xi}_h^\theta,\boldsymbol{\eta}_h)_{\mathcal{T}_h}+\lambda^{-1}t^2(\boldsymbol{\xi}_h^\gamma,\boldsymbol{\eta}_h)_{\mathcal{T}_h}. \tag{18}$$

*Proof.* Since $\boldsymbol{\gamma}=\lambda t^{-2}(\nabla w-\boldsymbol{\theta})$, we have

$$\boldsymbol{\Pi}_k^o\boldsymbol{\gamma}=\lambda t^{-2}\boldsymbol{\Pi}_k^o(\nabla w-\boldsymbol{\theta})=\lambda t^{-2}(\boldsymbol{\Pi}_k^o\nabla w-\boldsymbol{\Pi}_k^o\boldsymbol{\theta}).$$

Taking $\boldsymbol{\tau}_h=\mathbf{0}$ in (11a) yields

$$\lambda^{-1}t^2(\boldsymbol{\gamma}_h,\boldsymbol{\eta}_h)_{\mathcal{T}_h}=-(w_h,\nabla\cdot\boldsymbol{\eta}_h)_{\mathcal{T}_h}+\langle\widehat{w}_h,\nabla\cdot\boldsymbol{\eta}_h\rangle_{\partial\mathcal{T}_h}-(\boldsymbol{\theta}_h,\boldsymbol{\eta}_h)_{\mathcal{T}_h},\quad\forall\boldsymbol{\eta}_h\in\boldsymbol{\Gamma}_h.$$

The two relations above, together with integration by parts, imply

$$\begin{aligned}(\boldsymbol{\xi}_h^{\gamma},\boldsymbol{\eta}_h)_{\mathcal{T}_h} &= (\boldsymbol{\Pi}_k^o\boldsymbol{\gamma}-\boldsymbol{\gamma}_h,\boldsymbol{\eta}_h)_{\mathcal{T}_h}\\ &= \lambda t^{-2}(\boldsymbol{\Pi}_k^o\nabla w-\boldsymbol{\Pi}_k^o\boldsymbol{\theta},\boldsymbol{\eta}_h)_{\mathcal{T}_h}-\lambda t^{-2}\left[-(w_h,\nabla\cdot\boldsymbol{\eta}_h)_{\mathcal{T}_h}+\langle\widehat{w}_h,\nabla\cdot\boldsymbol{\eta}_h\rangle_{\partial\mathcal{T}_h}-(\boldsymbol{\theta}_h,\boldsymbol{\eta}_h)_{\mathcal{T}_h}\right]\\ &= \lambda t^{-2}\left[-(\xi_h^{w},\nabla\cdot\boldsymbol{\eta}_h)_{\mathcal{T}_h}+\langle\xi_h^{\widehat{w}},\nabla\cdot\boldsymbol{\eta}_h\rangle_{\partial\mathcal{T}_h}-(\boldsymbol{\xi}_h^{\boldsymbol{\theta}},\boldsymbol{\eta}_h)_{\mathcal{T}_h}\right],\end{aligned}$$

which indicates

$$-(\xi_h^{w},\nabla\cdot\boldsymbol{\eta}_h)_{\mathcal{T}_h}+\langle\xi_h^{\widehat{w}},\nabla\cdot\boldsymbol{\eta}_h\rangle_{\partial\mathcal{T}_h}=(\boldsymbol{\xi}_h^{\boldsymbol{\theta}},\boldsymbol{\eta}_h)_{\mathcal{T}_h}+\lambda^{-1}t^2(\boldsymbol{\xi}_h^{\gamma},\boldsymbol{\eta}_h)_{\mathcal{T}_h}.$$

This completes the proof. □

In what follows we suppose that the following regularity result holds:

$$\|\boldsymbol{\theta}\|_{k+1}+\|\boldsymbol{\sigma}\|_k+\|r\|_{k+1}+\|p\|_k+t\|p\|_{k+1}+\|w\|_{k+1}\lesssim\|\boldsymbol{f}\|_{k-1}+\|g\|_{k-1}. \tag{19}$$

From Theorem 2.1 we know that (19) holds true when $k=1$.

**Lemma 4.3.** *Let $(\boldsymbol{\sigma},\boldsymbol{\gamma},\boldsymbol{\theta},w)\in([L^2(\Omega)]^{2\times2}\cap\mathbb{S})\times[L^2(\Omega)]^2\times[H_0^1(\Omega)]^2\times H_0^1(\Omega)$ be the weak solution to problem* (5) *with boundary condition* (2) *and $(\boldsymbol{\sigma}_h,\boldsymbol{\gamma}_h,\boldsymbol{\theta}_h,\widehat{\boldsymbol{\theta}}_h,w_h,\widehat{w}_h)\in\boldsymbol{\Sigma}_h\times\boldsymbol{\Gamma}_h\times\boldsymbol{\Theta}_h\times\widehat{\boldsymbol{\Theta}}_h^0\times W_h\times\widehat{W}_h^0$ be the solution to the HDG scheme* (11). *Then, under the regularity condition* (19)*, the following error estimate holds:*

$$\|\boldsymbol{\xi}_h^{\sigma}\|_{\mathcal{T}_h}+t\|\boldsymbol{\xi}_h^{\gamma}\|_{\mathcal{T}_h}+\|(\boldsymbol{\xi}_h^{\theta},\boldsymbol{\xi}_h^{\widehat{\theta}})\|_{\Theta}+\|(\xi_h^{w},\xi_h^{\widehat{w}})\|_{W}\lesssim h^k\left(\|\boldsymbol{f}\|_{k-1}+\|g\|_{k-1}\right). \tag{20}$$

*Proof.* Subtract (11a) and (11b) from (17a) and (17b), respectively, then we have the following error equations:

$$\begin{cases}a_h(\boldsymbol{\xi}_h^{\sigma},\boldsymbol{\xi}_h^{\gamma};\boldsymbol{\tau}_h,\boldsymbol{\eta}_h)-b_h(\boldsymbol{\tau}_h,\boldsymbol{\eta}_h;\boldsymbol{\xi}_h^{\theta},\boldsymbol{\xi}_h^{\widehat{\theta}},\xi_h^{w},\xi_h^{\widehat{w}})=0,\\ b_h(\boldsymbol{\xi}_h^{\sigma},\boldsymbol{\xi}_h^{\gamma};\boldsymbol{\beta}_h,\widehat{\boldsymbol{\beta}}_h,v_h,\widehat{v}_h)+s_h(\boldsymbol{\xi}_h^{\theta},\boldsymbol{\xi}_h^{\widehat{\theta}},\xi_h^{w},\xi_h^{\widehat{w}};\boldsymbol{\beta}_h,\widehat{\boldsymbol{\beta}}_h,v_h,\widehat{v}_h)=E(\boldsymbol{\beta}_h,\widehat{\boldsymbol{\beta}}_h,v_h,\widehat{v}_h)\end{cases} \tag{21}$$

for all $(\boldsymbol{\tau}_h,\boldsymbol{\eta}_h,\boldsymbol{\beta}_h,\widehat{\boldsymbol{\beta}}_h,v_h,\widehat{v}_h)\in\boldsymbol{\Sigma}_h\times\boldsymbol{\Gamma}_h\times\boldsymbol{\Theta}_h\times\widehat{\boldsymbol{\Theta}}_h^0\times W_h\times\widehat{W}_h^0$. Take $(\boldsymbol{\tau}_h,\boldsymbol{\eta}_h,\boldsymbol{\beta}_h,\widehat{\boldsymbol{\beta}}_h,v_h,\widehat{v}_h)=(\boldsymbol{\xi}_h^{\sigma},\boldsymbol{\xi}_h^{\gamma},\boldsymbol{\xi}_h^{\theta},\boldsymbol{\xi}_h^{\widehat{\theta}},\xi_h^{w},\xi_h^{\widehat{w}})$ in (21) and add the two equations together to get

$$a_h(\boldsymbol{\xi}_h^{\sigma},\boldsymbol{\xi}_h^{\gamma};\boldsymbol{\xi}_h^{\sigma},\boldsymbol{\xi}_h^{\gamma})+s_h(\boldsymbol{\xi}_h^{\theta},\boldsymbol{\xi}_h^{\widehat{\theta}},\xi_h^{w},\xi_h^{\widehat{w}};\boldsymbol{\xi}_h^{\theta},\boldsymbol{\xi}_h^{\widehat{\theta}},\xi_h^{w},\xi_h^{\widehat{w}})=E(\boldsymbol{\xi}_h^{\theta},\boldsymbol{\xi}_h^{\widehat{\theta}},\xi_h^{w},\xi_h^{\widehat{w}}). \tag{22}$$

By (21) and the LBB condition in Theorem 3.1 we obtain

$$\begin{aligned}\|(\boldsymbol{\xi}_h^{\theta},\boldsymbol{\xi}_h^{\widehat{\theta}})\|_{\Theta}+\|(\xi_h^{w},\xi_h^{\widehat{w}})\|_{W}&\lesssim\sup_{\mathbf{0}\neq(\boldsymbol{\tau}_h,\boldsymbol{\eta}_h)\in\boldsymbol{\Sigma}_h\times\boldsymbol{\Gamma}_h}\frac{b_h(\boldsymbol{\tau}_h,\boldsymbol{\eta}_h;\boldsymbol{\xi}_h^{\theta},\boldsymbol{\xi}_h^{\widehat{\theta}},\xi_h^{w},\xi_h^{\widehat{w}})}{\|\boldsymbol{\tau}_h\|_{\mathcal{T}_h}+t\|\boldsymbol{\eta}_h\|_{\mathcal{T}_h}}+s_h(\boldsymbol{\xi}_h^{\theta},\boldsymbol{\xi}_h^{\widehat{\theta}},\xi_h^{w},\xi_h^{\widehat{w}};\boldsymbol{\xi}_h^{\theta},\boldsymbol{\xi}_h^{\widehat{\theta}},\xi_h^{w},\xi_h^{\widehat{w}})^{1/2}\\ &\lesssim a_h(\boldsymbol{\xi}_h^{\sigma},\boldsymbol{\xi}_h^{\gamma};\boldsymbol{\xi}_h^{\sigma},\boldsymbol{\xi}_h^{\gamma})^{1/2}+s_h(\boldsymbol{\xi}_h^{\theta},\boldsymbol{\xi}_h^{\widehat{\theta}},\xi_h^{w},\xi_h^{\widehat{w}};\boldsymbol{\xi}_h^{\theta},\boldsymbol{\xi}_h^{\widehat{\theta}},\xi_h^{w},\xi_h^{\widehat{w}})^{1/2},\end{aligned}$$

which, together with (6), (22) and the definition of $a_h$, gives

$$\|\boldsymbol{\xi}_h^{\sigma}\|_{\mathcal{T}_h}^2+t^2\|\boldsymbol{\xi}_h^{\gamma}\|_{\mathcal{T}_h}^2+\|(\boldsymbol{\xi}_h^{\theta},\boldsymbol{\xi}_h^{\widehat{\theta}})\|_{\Theta}^2+\|(\xi_h^{w},\xi_h^{\widehat{w}})\|_{W}^2\lesssim E(\boldsymbol{\xi}_h^{\theta},\boldsymbol{\xi}_h^{\widehat{\theta}},\xi_h^{w},\xi_h^{\widehat{w}}).$$

By the definition of $E(\cdot,\cdot,\cdot,\cdot)$, we write $E(\boldsymbol{\xi}_h^{\theta},\boldsymbol{\xi}_h^{\widehat{\theta}},\xi_h^{w},\xi_h^{\widehat{w}})=\sum_{i=1}^4E_i$ with

$$\begin{aligned}E_1&=\langle\alpha(\boldsymbol{\Pi}_{\ell}^{\partial}\boldsymbol{\Pi}_k^o\boldsymbol{\theta}-\boldsymbol{\Pi}_{\ell}^{\partial}\boldsymbol{\theta}),\boldsymbol{\Pi}_{\ell}^{\partial}\boldsymbol{\xi}_h^{\theta}-\boldsymbol{\xi}_h^{\widehat{\theta}}\rangle_{\partial\mathcal{T}_h}+\langle\alpha(\Pi_k^o w-\Pi_k^{\partial}w),v_h-\widehat{v}_h\rangle_{\partial\mathcal{T}_h},\\ E_2&=-(\xi_h^{w},\nabla\cdot\boldsymbol{\Pi}_k^o\nabla^{\perp}p)_{\mathcal{T}_h}+\langle\xi_h^{\widehat{w}},\boldsymbol{n}\cdot\boldsymbol{\Pi}_k^o\nabla^{\perp}p\rangle_{\partial\mathcal{T}_h},\\ E_3&=\langle\boldsymbol{\xi}_h^{\widehat{\theta}}-\boldsymbol{\xi}_h^{\theta},\boldsymbol{\Pi}_m^o\boldsymbol{\sigma}\boldsymbol{n}-\boldsymbol{\sigma}\boldsymbol{n}\rangle_{\partial\mathcal{T}_h},\\ E_4&=\langle\xi_h^{\widehat{w}}-\xi_h^{w},\boldsymbol{\Pi}_k^o\nabla r\cdot\boldsymbol{n}-\nabla r\cdot\boldsymbol{n}\rangle_{\partial\mathcal{T}_h},\end{aligned}$$

and estimate them one by one. For the term $E_1$ we have

$$E_1=\langle\alpha(\boldsymbol{\Pi}_k^o\boldsymbol{\theta}-\boldsymbol{\theta}),\boldsymbol{\Pi}_{\ell}^{\partial}\boldsymbol{\xi}_h^{\theta}-\boldsymbol{\xi}_h^{\widehat{\theta}}\rangle_{\partial\mathcal{T}_h}+\langle\alpha(\Pi_k^o w-w),v_h-\widehat{v}_h\rangle_{\partial\mathcal{T}_h}\lesssim h^k(|\boldsymbol{\theta}|_{k+1}+|w|_{k+1})s_h(\boldsymbol{\xi}_h^{\theta},\boldsymbol{\xi}_h^{\widehat{\theta}},\xi_h^{w},\xi_h^{\widehat{w}};\boldsymbol{\xi}_h^{\theta},\boldsymbol{\xi}_h^{\widehat{\theta}},\xi_h^{w},\xi_h^{\widehat{w}})^{1/2}.$$

It is well known that there exists an interpolation $\mathcal{I}_h:H^1(\Omega)\to H^1(\Omega)\cap\mathbb{P}_{k+1}(\mathcal{T}_h)$ such that for all $p\in H^s(\Omega)$ with $1\le s\le k+1$, it holds the approximation property

$$\|p-\mathcal{I}_hp\|_{\mathcal{T}_h}+h|p-\mathcal{I}_hp|_1\lesssim h^s|p|_s,\quad 1\le s\le k+1, \tag{23}$$

where $\mathbb{P}_{k+1}(\mathcal{T}_h)$ is the set of piecewise polynomials on $\mathcal{T}_h$ of degree at most $k+1$. Then we apply (18), integration by parts and (23) to get

$$\begin{aligned}
E_2 &= -(\xi_h^w, \nabla\cdot(\mathbf{\Pi}_k^o\nabla^\perp p - \nabla^\perp\mathcal{I}_h p))_{\mathcal{T}_h} + \langle \xi_h^{\widehat{w}}, \boldsymbol{n}\cdot(\mathbf{\Pi}_k^o\nabla^\perp p - \nabla^\perp\mathcal{I}_h p)\rangle_{\partial\mathcal{T}_h}\\
&= (\lambda^{-1}t^2\boldsymbol{\xi}_h^\gamma + \boldsymbol{\xi}_h^\theta, \nabla^\perp(p-\mathcal{I}_h p))_{\mathcal{T}_h}\\
&= (\lambda^{-1}t^2\boldsymbol{\xi}_h^\gamma, \nabla^\perp(p-\mathcal{I}_h p))_{\mathcal{T}_h} - (\nabla^\perp\cdot\boldsymbol{\xi}_h^\theta, p-\mathcal{I}_h p)_{\mathcal{T}_h} + \langle \boldsymbol{n}\cdot(\boldsymbol{\xi}_h^\theta - \boldsymbol{\xi}_h^{\widehat{\theta}}), p-\mathcal{I}_h p\rangle_{\partial\mathcal{T}_h}\\
&\lesssim h^k t^2\|\boldsymbol{\xi}_h^\gamma\|_{\mathcal{T}_h}|p|_{k+1} + h^k\left(\sum_{T\in\mathcal{T}_h} h_T^{-1}\|\mathbf{\Pi}_\ell^\partial\boldsymbol{\xi}_h^\theta - \boldsymbol{\xi}_h^{\widehat{\theta}}\|_{\partial T}^2\right)^{1/2}|p|_k + h^k\|\nabla\boldsymbol{\xi}_h^\theta\|_{\mathcal{T}_h}|p|_k\\
&\lesssim h^k(t|p|_{k+1} + |p|_k)(t\|\boldsymbol{\xi}_h^\gamma\|_{\mathcal{T}_h} + \|(\boldsymbol{\xi}_h^\theta, \boldsymbol{\xi}_h^{\widehat{\theta}})\|_\Theta).
\end{aligned} \tag{24}$$

From Cauchy-Schwarz's inequality and Lemma 2.1, it follows that

$$\begin{aligned}
E_3 =&\langle \boldsymbol{\xi}_h^{\widehat{\theta}} - \boldsymbol{\xi}_h^\theta, \mathbf{\Pi}_m^o\boldsymbol{\sigma}\boldsymbol{n} - \boldsymbol{\sigma}\boldsymbol{n}\rangle_{\partial\mathcal{T}_h}\\
=&\langle \boldsymbol{\xi}_h^{\widehat{\theta}} - \mathbf{\Pi}_\ell^\partial\boldsymbol{\xi}_h^\theta, \mathbf{\Pi}_m^o\boldsymbol{\sigma}\boldsymbol{n} - \boldsymbol{\sigma}\boldsymbol{n}\rangle_{\partial\mathcal{T}_h} + \langle \mathbf{\Pi}_\ell^\partial\boldsymbol{\xi}_h^\theta - \boldsymbol{\xi}_h^\theta, \mathbf{\Pi}_m^o\boldsymbol{\sigma}\boldsymbol{n} - \boldsymbol{\sigma}\boldsymbol{n}\rangle_{\partial\mathcal{T}_h}\\
\lesssim& h^k|\boldsymbol{\sigma}|_k\|(\boldsymbol{\xi}_h^\theta, \boldsymbol{\xi}_h^{\widehat{\theta}})\|_\Theta
\end{aligned}$$

and

$$E_4 = \langle \xi_h^{\widehat{w}} - \xi_h^w, \mathbf{\Pi}_k^o\nabla r\cdot\boldsymbol{n} - \nabla r\cdot\boldsymbol{n}\rangle_{\partial\mathcal{T}_h} \lesssim h^k|r|_{k+1}\|\alpha^{1/2}(\xi_h^{\widehat{w}} - \xi_h^w)\|_{\partial\mathcal{T}_h}.$$

Combining the above estimates of $E_i$, we get

$$\begin{aligned}
&\|\boldsymbol{\xi}_h^\sigma\|_{\mathcal{T}_h}^2 + t^2\|\boldsymbol{\xi}_h^\gamma\|_{\mathcal{T}_h}^2 + \|(\boldsymbol{\xi}_h^\theta, \boldsymbol{\xi}_h^{\widehat{\theta}})\|_\Theta^2 + \|(\xi_h^w, \xi_h^{\widehat{w}})\|_W^2\\
\lesssim& h^k(|\boldsymbol{\theta}|_{k+1} + |w|_{k+1} + |r|_{k+1} + t|p|_{k+1} + |p|_k + |\boldsymbol{\sigma}|_k)\left(t\|\boldsymbol{\xi}_h^\gamma\|_{\mathcal{T}_h} + \|(\boldsymbol{\xi}_h^\theta, \boldsymbol{\xi}_h^{\widehat{\theta}})\|_\Theta + \|(\xi_h^w, \xi_h^{\widehat{w}})\|_W\right),
\end{aligned}$$

which, together with (19), leads to the desired conclusion. □

Finally, in light of Lemma 4.3 and the triangle inequality, we easily obtain the following error estimate:

**Theorem 4.1.** *Under the conditions of Lemma 4.3, it holds*

$$\|\boldsymbol{\sigma} - \boldsymbol{\sigma}_h\|_{\mathcal{T}_h} + \|\nabla\boldsymbol{\theta} - \nabla\boldsymbol{\theta}_h\|_{\mathcal{T}_h} + \|\nabla w - \nabla w_h\|_{\mathcal{T}_h} + t\|\boldsymbol{\gamma} - \boldsymbol{\gamma}_h\|_{\mathcal{T}_h} \lesssim h^k\left(\|\boldsymbol{f}\|_{k-1} + \|g\|_{k-1}\right).$$

### *4.2. $L^2$ error estimate*

In order to derive the $L^2$-error estimation for the transverse displacement and rotation approximations, we shall perform the Aubin-Nitsche duality argument. To this end, we introduce an auxiliary problem:

$$\begin{cases}
\mathcal{C}^{-1}\boldsymbol{\varsigma} - \boldsymbol{\epsilon}(\boldsymbol{\vartheta}) = 0 & \text{in } \Omega,\\
-\nabla\cdot\boldsymbol{\varsigma} - \boldsymbol{\phi} = \boldsymbol{\xi}_h^\theta & \text{in } \Omega,\\
-\nabla\cdot\boldsymbol{\phi} = \xi_h^w & \text{in } \Omega,\\
\lambda^{-1}t^2\boldsymbol{\phi} - (\nabla\psi - \boldsymbol{\vartheta}) = 0 & \text{in } \Omega,\\
\boldsymbol{\vartheta} = \boldsymbol{0}, \quad \psi = 0 & \text{on } \partial\Omega.
\end{cases} \tag{25}$$

When $\Omega$ is a convex polygon or a smoothly bounded domain, by Theorem 2.1 we have

$$\|\boldsymbol{\varsigma}\|_1 + \|\boldsymbol{\vartheta}\|_2 + \|\boldsymbol{\phi}\|_{\mathcal{T}_h} + t\|\boldsymbol{\phi}\|_1 + \|\psi\|_2 + \|s\|_2 + \|q\|_1 + t\|q\|_1 \lesssim \|\boldsymbol{\xi}_h^\theta\|_{\mathcal{T}_h} + \|\xi_h^w\|_{\mathcal{T}_h}, \tag{26}$$

where $s\in H_0^1(\Omega)$, $q\in H^1(\Omega)\cap L_0^2(\Omega)$ satisfy the Helmholtz decomposition of $\boldsymbol{\psi}$, i.e. $\boldsymbol{\psi} = \nabla s + \nabla^\perp q$.

We are now ready to show the $L^2$-error estimation for the rotation and displacement.

**Theorem 4.2.** *Under the regularity assumption* (26) *and the conditions of Lemma 4.3, it holds*

$$\|\boldsymbol{\theta} - \boldsymbol{\theta}_h\|_{\mathcal{T}_h} + \|w - w_h\|_{\mathcal{T}_h} \lesssim h^{k+1}(\|\boldsymbol{f}\|_{k-1} + \|g\|_{k-1}).$$

*Proof.* Similar to Lemma 4.1, for all $(\boldsymbol{\tau}_h, \boldsymbol{\eta}_h, \boldsymbol{\beta}_h, \widehat{\boldsymbol{\beta}}_h, v_h, \widehat{v}_h) \in \boldsymbol{\Sigma}_h \times \boldsymbol{\Gamma}_h \times \boldsymbol{\Theta}_h \times \widehat{\boldsymbol{\Theta}}_h^0 \times W_h \times \widehat{W}_h^0$, we can get

$$a_h(\boldsymbol{\Pi}_k^o\boldsymbol{\varsigma}, \boldsymbol{\Pi}_k^o\boldsymbol{\phi}; \boldsymbol{\tau}_h, \boldsymbol{\eta}_h) - b_h(\boldsymbol{\tau}_h, \boldsymbol{\eta}_h; \boldsymbol{\Pi}_k^o\boldsymbol{\vartheta}, \boldsymbol{\Pi}_\ell^\partial\boldsymbol{\vartheta}, \Pi_k^o\psi, \Pi_k^\partial\psi) = 0, \tag{27}$$

$$b_h(\boldsymbol{\Pi}_k^o\boldsymbol{\varsigma}, \boldsymbol{\Pi}_k^o\boldsymbol{\phi}; \boldsymbol{\beta}_h, \widehat{\boldsymbol{\beta}}_h, v_h, \widehat{v}_h) + s_h(\boldsymbol{\Pi}_k^o\boldsymbol{\vartheta}, \boldsymbol{\Pi}_\ell^\partial\boldsymbol{\vartheta}, \Pi_k^o\psi, \Pi_k^\partial\psi; \boldsymbol{\beta}_h, \widehat{\boldsymbol{\beta}}_h, v_h, \widehat{v}_h) = (\boldsymbol{\xi}_h^\theta, \boldsymbol{\beta}_h)_{\mathcal{T}_h} + (\xi_h^w, v_h)_{\mathcal{T}_h} + E^*(\boldsymbol{\beta}_h, \widehat{\boldsymbol{\beta}}_h, v_h, \widehat{v}_h), \tag{28}$$

where

$$\begin{aligned} E^*(\boldsymbol{\beta}_h, \widehat{\boldsymbol{\beta}}_h, v_h, \widehat{v}_h) :=& s_h(\boldsymbol{\Pi}_k^o\boldsymbol{\vartheta}, \boldsymbol{\Pi}_\ell^\partial\boldsymbol{\vartheta}, \Pi_k^o\psi, \Pi_k^\partial\psi; \boldsymbol{\beta}_h, \widehat{\boldsymbol{\beta}}_h, v_h, \widehat{v}_h) + [-(v_h, \nabla\cdot\boldsymbol{\Pi}_k^o\nabla^\perp q)_{\mathcal{T}_h} + \langle v_h, \boldsymbol{n}\cdot\boldsymbol{\Pi}_k^o\nabla^\perp q\rangle_{\partial\mathcal{T}_h}] \\ &+ \langle\widehat{\boldsymbol{\beta}}_h - \boldsymbol{\beta}_h, \boldsymbol{\Pi}_m^o\boldsymbol{\varsigma}\boldsymbol{n} - \boldsymbol{\varsigma}\boldsymbol{n}\rangle_{\partial\mathcal{T}_h} + \langle\widehat{v}_h - v_h, \boldsymbol{\Pi}_k^o\nabla s\cdot\boldsymbol{n} - \nabla s\cdot\boldsymbol{n}\rangle_{\partial\mathcal{T}_h}. \end{aligned}$$

Then we have

$$\begin{aligned} \|\boldsymbol{\xi}_h^\theta\|_{\mathcal{T}_h}^2 + \|\xi_h^w\|_{\mathcal{T}_h}^2 =& b_h(\boldsymbol{\Pi}_k^o\boldsymbol{\varsigma}, \boldsymbol{\Pi}_k^o\boldsymbol{\phi}; \boldsymbol{\xi}_h^\theta, \widehat{\boldsymbol{\xi}_h^\theta}, \xi_h^w, \widehat{\xi_h^w}) + s_h(\boldsymbol{\Pi}_k^o\boldsymbol{\vartheta}, \boldsymbol{\Pi}_\ell^\partial\boldsymbol{\vartheta}, \Pi_k^o\psi, \Pi_k^\partial\psi; \boldsymbol{\xi}_h^\theta, \widehat{\boldsymbol{\xi}_h^\theta}, \xi_h^w, \widehat{\xi_h^w}) - E^*(\boldsymbol{\xi}_h^\theta, \widehat{\boldsymbol{\xi}_h^\theta}, \xi_h^w, \widehat{\xi_h^w}) \\ =& a_h(\boldsymbol{\Pi}_k^o\boldsymbol{\varsigma}, \boldsymbol{\Pi}_k^o\boldsymbol{\phi}; \boldsymbol{\xi}_h^\sigma, \boldsymbol{\xi}_h^\gamma) + s_h(\boldsymbol{\Pi}_k^o\boldsymbol{\vartheta}, \boldsymbol{\Pi}_\ell^\partial\boldsymbol{\vartheta}, \Pi_k^o\psi, \Pi_k^\partial\psi; \boldsymbol{\xi}_h^\theta, \widehat{\boldsymbol{\xi}_h^\theta}, \xi_h^w, \widehat{\xi_h^w}) - E^*(\boldsymbol{\xi}_h^\theta, \widehat{\boldsymbol{\xi}_h^\theta}, \xi_h^w, \widehat{\xi_h^w}) \\ =& E(\boldsymbol{\Pi}_k^o\boldsymbol{\vartheta}, \boldsymbol{\Pi}_\ell^\partial\boldsymbol{\vartheta}, \Pi_k^o\psi, \Pi_k^\partial\psi) - E^*(\boldsymbol{\xi}_h^\theta, \widehat{\boldsymbol{\xi}_h^\theta}, \xi_h^w, \widehat{\xi_h^w}). \end{aligned} \tag{29}$$

From the fact that $(\nabla\psi, \nabla^\perp p) = 0$ and the identity $\lambda^{-1}t^2\boldsymbol{\phi} - (\nabla\psi - \boldsymbol{\vartheta}) = 0$ in (25), it follows

$$\begin{aligned} -(\Pi_k^o\psi, \nabla\cdot\boldsymbol{\Pi}_k^o\nabla^\perp p)_{\mathcal{T}_h} + \langle\Pi_k^\partial\psi, \boldsymbol{n}\cdot\boldsymbol{\Pi}_k^o\nabla^\perp p\rangle_{\partial\mathcal{T}_h} =& -(\psi, \nabla\cdot\boldsymbol{\Pi}_k^o\nabla^\perp p)_{\mathcal{T}_h} + \langle\psi, \boldsymbol{n}\cdot\boldsymbol{\Pi}_k^o\nabla^\perp p\rangle_{\partial\mathcal{T}_h} \\ =& (\boldsymbol{\Pi}_k^o\nabla\psi - \nabla\psi, \nabla^\perp p - \boldsymbol{\Pi}_k^o\nabla^\perp p)_{\mathcal{T}_h} \\ =& (\lambda^{-1}t^2(\boldsymbol{\Pi}_k^o\boldsymbol{\phi} - \boldsymbol{\phi})_{\mathcal{T}_h} - (\boldsymbol{\Pi}_k^o\boldsymbol{\vartheta} - \boldsymbol{\vartheta}), \nabla^\perp p - \boldsymbol{\Pi}_k^o\nabla^\perp p)_{\mathcal{T}_h} \\ \lesssim& h^{k+1}(t^2|\boldsymbol{\phi}|_1|p|_{k+1} + |\boldsymbol{\vartheta}|_2|p|_k). \end{aligned}$$

Thus,

$$\begin{aligned} E(\boldsymbol{\Pi}_k^o\boldsymbol{\vartheta}, \boldsymbol{\Pi}_\ell^\partial\boldsymbol{\vartheta}, \Pi_k^o\psi, \Pi_k^\partial\psi) \lesssim& h^{k+1}(|w|_{k+1} + |r|_{k+1} + t|p|_{k+1} + |p|_k + |\boldsymbol{\sigma}|_k)(t|\boldsymbol{\phi}|_1 + |\boldsymbol{\vartheta}|_2 + |\psi|_2) \\ \lesssim& h^{k+1}(|w|_{k+1} + |r|_{k+1} + t|p|_{k+1} + |p|_k + |\boldsymbol{\sigma}|_k)(\|\boldsymbol{\xi}_h^\theta\|_{\mathcal{T}_h} + \|\xi_h^w\|_{\mathcal{T}_h}). \end{aligned} \tag{30}$$

We use the same estimation in (24) to get

$$(\xi_h^w, \nabla\cdot\boldsymbol{\Pi}_k^\partial\nabla^\perp q)_{\mathcal{T}_h} - \langle\xi_h^{\widehat{w}}, n\cdot\boldsymbol{\Pi}_k^\partial\nabla^\perp q\rangle_{\partial\mathcal{T}_h} \lesssim h(t|q|_2 + |q|_1)(t\|\boldsymbol{\xi}_h^\gamma\|_{\mathcal{T}_h} + \|(\boldsymbol{\xi}_h^\theta, \widehat{\boldsymbol{\xi}_h^\theta})\|_{\boldsymbol{\Theta}}),$$

which, together with the definition of $E^*(\cdot,\cdot,\cdot,\cdot)$, (26) and (20), yields

$$\begin{aligned} -E^*(\boldsymbol{\xi}_h^\theta, \widehat{\boldsymbol{\xi}_h^\theta}, \xi_h^w, \widehat{\xi_h^w}) \lesssim& s_h(\boldsymbol{\Pi}_k^o\boldsymbol{\vartheta}, \boldsymbol{\Pi}_\ell^\partial\boldsymbol{\vartheta}, \Pi_k^o\psi, \Pi_k^\partial\psi; \boldsymbol{\Pi}_k^o\boldsymbol{\vartheta}, \boldsymbol{\Pi}_\ell^\partial\boldsymbol{\vartheta}, \Pi_k^o\psi, \Pi_k^\partial\psi)^{1/2} s_h(\boldsymbol{\xi}_h^\theta, \widehat{\boldsymbol{\xi}_h^\theta}, \xi_h^w, \widehat{\xi_h^w}; \boldsymbol{\xi}_h^\theta, \widehat{\boldsymbol{\xi}_h^\theta}, \xi_h^w, \widehat{\xi_h^w})^{1/2} \\ &+ h(t|q|_2 + |q|_1)(t\|\boldsymbol{\xi}_h^\gamma\|_{\mathcal{T}_h} + \|(\boldsymbol{\xi}_h^\theta, \widehat{\boldsymbol{\xi}_h^\theta})\|_{\boldsymbol{\Theta}}) + h|\boldsymbol{\varsigma}|_1\|(\boldsymbol{\xi}_h^\theta, \widehat{\boldsymbol{\xi}_h^\theta})\|_{\boldsymbol{\Theta}} + h|s|_2\|(\xi_h^w, \widehat{\xi_h^w})\|_W \\ \lesssim& h(t|q|_2 + |q|_1)(t\|\boldsymbol{\xi}_h^\gamma\|_{\mathcal{T}_h} + \|(\boldsymbol{\xi}_h^\theta, \widehat{\boldsymbol{\xi}_h^\theta})\|_{\boldsymbol{\Theta}}) + h(|\boldsymbol{\vartheta}|_2 + |\psi|_2 + |\boldsymbol{\varsigma}|_1 + |s|_2)(\|(\boldsymbol{\xi}_h^\theta, \widehat{\boldsymbol{\xi}_h^\theta})\|_{\boldsymbol{\Theta}} + \|(\xi_h^w, \widehat{\xi_h^w})\|_W) \\ \lesssim& h^{k+1}(\|\boldsymbol{\xi}_h^\theta\|_{\mathcal{T}_h} + \|\xi_h^w\|_{\mathcal{T}_h})(|\boldsymbol{\theta}|_{k+1} + |w|_{k+1} + |r|_{k+1} + t|p|_{k+1} + |p|_k + |\boldsymbol{\sigma}|_k). \end{aligned} \tag{31}$$

The desired conclusion follows from (29), (30), (31), the triangle inequality and the assumption (19). □

# 5. Numerical experiments

This section provides some numerical results to verify the performance of the HDG scheme (11). Although the theoretical results are obtained only on conforming triangles meshes, the numerical experiments are performed on quadrangle and nonconforming meshes as well. All tests are programmed in C++ using the Eigen[32] library.

## 5.1. *Square plate I*

We compute a square plate with analytical solution to show the convergence. This example is taken from[36]. The domain $\Omega$ is the unit square $(0,1)^2$, the material parameters are taken as $E = 1.0$, $\nu = 0.3$ and $\kappa = \frac{5}{6}$, and the HC boundary condition (2) is considered. The exact solution $(\boldsymbol{\theta}, w)$ of (1) is of the form

$$\begin{cases} \boldsymbol{\theta} = \left(100y^3(y-1)^3x^2(x-1)^2(2x-1),\ 100x^3(x-1)^3y^2(y-1)^2(2y-1)\right)^T, \\ w = 100\left(\frac{1}{3}x^3(x-1)^3y^3(y-1)^3 - \frac{2t^2}{5(1-\nu)}[y^3(y-1)^3x(x-1)(5x^2-5x+1) + x^3(x-1)^3y(y-1)(5y^2-5y+1)]\right). \end{cases}$$

Therefore, the body force and the transverse loading are

$$\begin{cases} \boldsymbol{f} = (0,0)^T, \\ g = \left(x^3(x-1)^3(5y^2-5y+1) + y^3(y-1)^3(5x^2-5x+1) + x(x-1)y(y-1)(5x^2-5x+1)(5y^2-5y+1)\right), \end{cases} \tag{32}$$

where $D = \frac{E}{12(1-\nu^2)}$.

Three types of meshes are shown in Figs. 1-3. We compute two cases with the pane thick $t = 1$ and $t = 10^{-10}$. The results are listed in Tables 1-6. From the results we can see that our HDG scheme (11), with $k = 1, 2, 3$, yields optimal convergence rates which are uniform with respect to the plane thickness $t$, i.e. $k-$th order rate for $\|\boldsymbol{\sigma} - \boldsymbol{\sigma}_h\|_{\mathcal{T}_h}$, $\|\nabla\boldsymbol{\theta} - \nabla\boldsymbol{\theta}_h\|_{\mathcal{T}_h}$, $\|\nabla w - \nabla w_h\|_{\mathcal{T}_h}$ and $t\|\boldsymbol{\gamma} - \boldsymbol{\gamma}_h\|_{\mathcal{T}_h}$, and $(k+1)-$th order rate for $\|\boldsymbol{\theta} - \boldsymbol{\theta}_h\|_{\mathcal{T}_h}$ and $\|w - w_h\|_{\mathcal{T}_h}$. These are conformable to the theoretical results of Theorems 4.1-4.2.

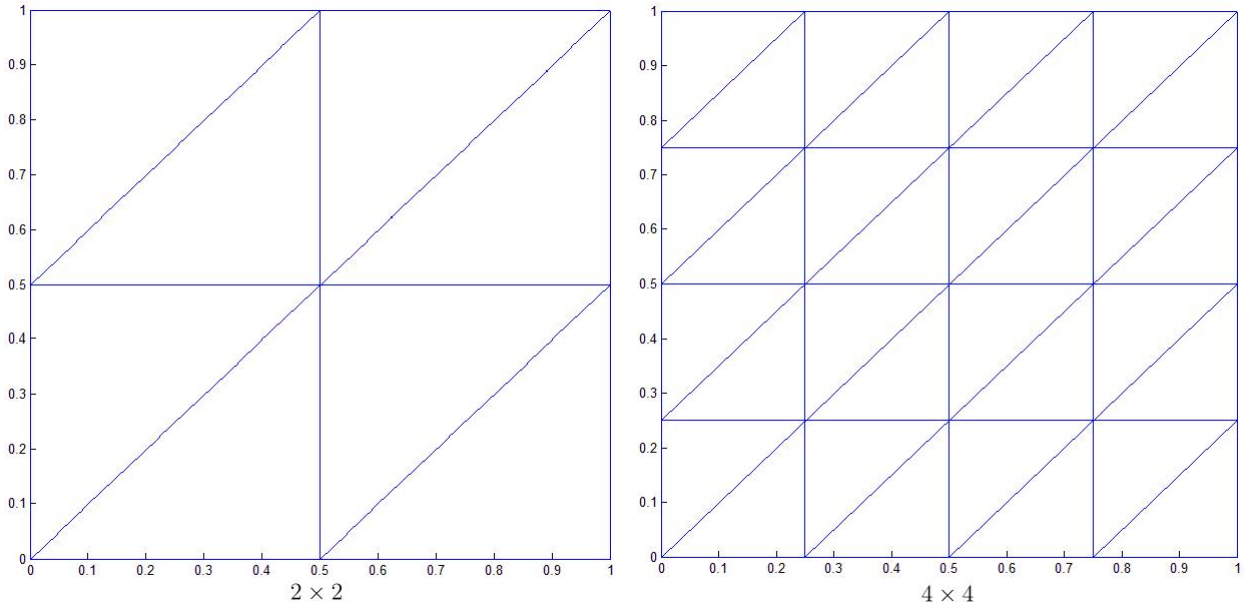


**Fig. 1.** Triangle meshes for square plate

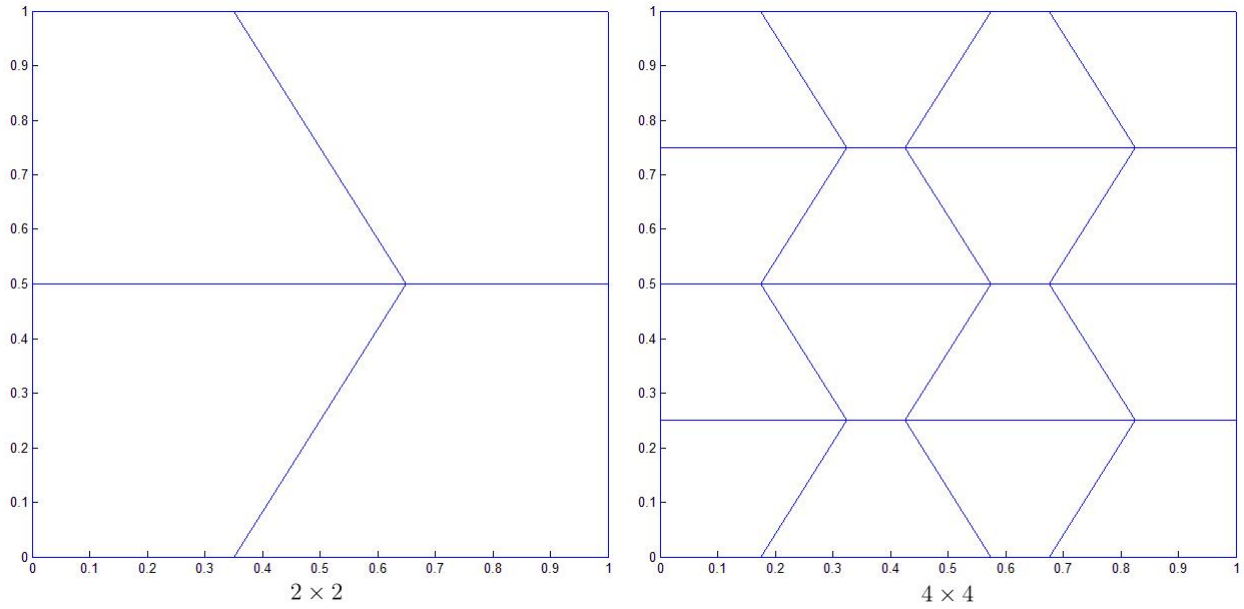


**Fig. 2.** Ladder-shaped meshes for square plate

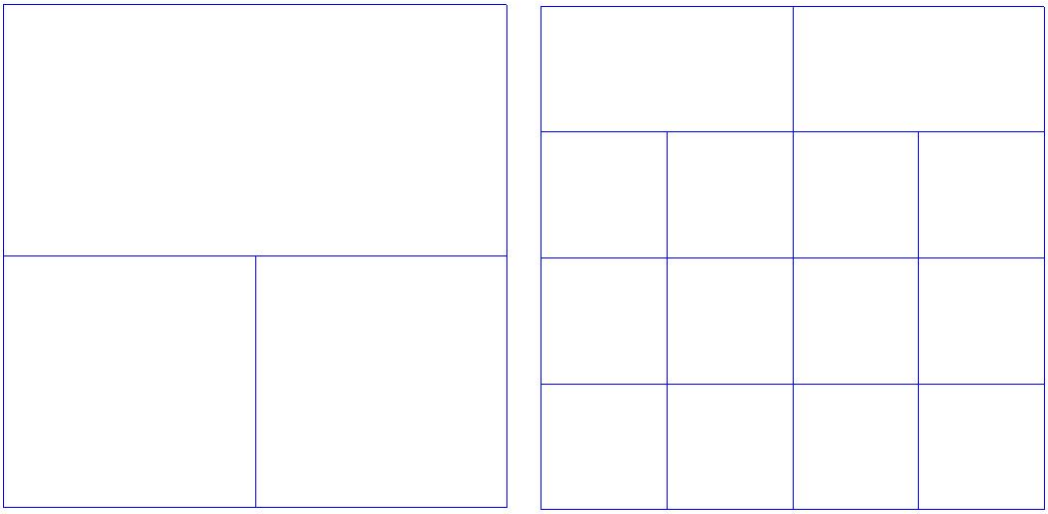


**Fig. 3.** Nonconforming quadrangle meshes for square plate

**Table 1.** Results for $k = l = m = 1$ with $t = 1$: Triangle meshes

| Mesh | $\frac{\|\boldsymbol{\theta}-\boldsymbol{\theta}_h\|_{\mathcal{T}_h}}{\|\boldsymbol{\theta}\|_{\mathcal{T}_h}}$ | | $\frac{\|\nabla\boldsymbol{\theta}-\nabla\boldsymbol{\theta}_h\|_{\mathcal{T}_h}}{\|\nabla\boldsymbol{\theta}\|_{\mathcal{T}_h}}$ | | $\frac{\|\boldsymbol{\sigma}-\boldsymbol{\sigma}_h\|_{\mathcal{T}_h}}{\|\boldsymbol{\sigma}\|_{\mathcal{T}_h}}$ | |
|---|---|---|---|---|---|---|
| | Error | Rate | Error | Rate | Error | Rate |
| $4 \times 4$ | 2.9721E-01 | | 5.5297E-01 | | 3.9414E-01 | |
| $8 \times 8$ | 9.7762E-02 | 1.60 | 3.3619E-01 | 0.72 | 1.9373E-01 | 1.02 |
| $16 \times 16$ | 2.6467E-02 | 1.89 | 1.7776E-01 | 0.92 | 9.5498E-02 | 1.02 |
| $32 \times 32$ | 6.7567E-03 | 1.97 | 9.0160E-02 | 0.98 | 4.7520E-02 | 1.01 |
| $64 \times 64$ | 1.6982E-03 | 1.99 | 4.5243E-02 | 0.99 | 2.3729E-02 | 1.00 |
| $128 \times 128$ | 4.2511E-04 | 2.00 | 2.2642E-02 | 1.00 | 1.1861E-02 | 1.00 |
| Mesh | $\frac{\|w-w_h\|_{\mathcal{T}_h}}{\|w\|_0}$ | | $\frac{\|\nabla w-\nabla w_h\|_{\mathcal{T}_h}}{\|\nabla w\|_0}$ | | $\frac{(t+h)\|\gamma-\gamma_h\|_{\mathcal{T}_h}}{\|\gamma\|_0}$ | |
| | Error | Rate | Error | Rate | Error | Rate |
| $4 \times 4$ | 2.6245E-01 | | 9.9710E-01 | | 3.8978E-01 | |
| $8 \times 8$ | 7.7770E-02 | 1.75 | 5.7070E-01 | 0.80 | 1.5503E-01 | 1.33 |
| $16 \times 16$ | 2.0450E-02 | 1.93 | 2.9689E-01 | 0.94 | 6.9436E-02 | 1.16 |
| $32 \times 32$ | 5.1820E-03 | 1.98 | 1.4974E-01 | 0.99 | 3.3179E-02 | 1.07 |
| $64 \times 64$ | 1.3000E-03 | 1.99 | 7.5026E-02 | 1.00 | 1.6272E-02 | 1.03 |
| $128 \times 128$ | 3.2529E-04 | 2.00 | 3.7533E-02 | 1.00 | 8.0651E-03 | 1.01 |

**Table 2.** Results for $k = l = m = 1$ with $t = 10^{-10}$: Triangle meshes

| Mesh | $\frac{\|\boldsymbol{\theta}-\boldsymbol{\theta}_h\|_{\mathcal{T}_h}}{\|\boldsymbol{\theta}\|_0}$ | | $\frac{\|\nabla\boldsymbol{\theta}-\nabla\boldsymbol{\theta}_h\|_{\mathcal{T}_h}}{\|\nabla\boldsymbol{\theta}\|_0}$ | | $\frac{\|\boldsymbol{\sigma}-\boldsymbol{\sigma}_h\|_{\mathcal{T}_h}}{\|\boldsymbol{\sigma}\|_0}$ | |
|---|---|---|---|---|---|---|
| | Error | Rate | Error | Rate | Error | Rate |
| $4 \times 4$ | 2.4099E-01 | | 5.2117E-01 | | 3.4890E-01 | |
| $8 \times 8$ | 7.5130E-02 | 1.68 | 3.2445E-01 | 0.68 | 1.8084E-01 | 0.95 |
| $16 \times 16$ | 1.8950E-02 | 1.99 | 1.7547E-01 | 0.89 | 9.3011E-02 | 0.96 |
| $32 \times 32$ | 4.6814E-03 | 2.02 | 8.9824E-02 | 0.97 | 4.7164E-02 | 0.98 |
| $64 \times 64$ | 1.1649E-03 | 2.01 | 4.5197E-02 | 0.99 | 2.3683E-02 | 0.99 |
| $128 \times 128$ | 2.9085E-04 | 2.00 | 2.2635E-02 | 1.00 | 1.1855E-02 | 1.00 |
| Mesh | $\frac{\|w-w_h\|_{\mathcal{T}_h}}{\|w\|_0}$ | | $\frac{\|\nabla w-\nabla w_h\|_{\mathcal{T}_h}}{\|\nabla w\|_0}$ | | $\frac{(t+h)\|\gamma-\gamma_h\|_{\mathcal{T}_h}}{\|\gamma\|_0}$ | |
| | Error | Rate | Error | Rate | Error | Rate |
| $4 \times 4$ | 1.1204E+00 | | 4.9179E+00 | | 2.5000E-01 | |
| $8 \times 8$ | 1.5803E-01 | 2.83 | 1.3865E+00 | 1.83 | 1.2500E-01 | 1.00 |
| $16 \times 16$ | 2.2226E-02 | 2.83 | 3.8571E-01 | 1.85 | 6.2500E-02 | 1.00 |
| $32 \times 32$ | 3.5818E-03 | 2.63 | 1.2377E-01 | 1.64 | 3.1250E-02 | 1.00 |
| $64 \times 64$ | 7.1592E-04 | 2.32 | 4.9418E-02 | 1.32 | 1.5625E-02 | 1.00 |
| $128 \times 128$ | 1.6578E-04 | 2.11 | 2.2879E-02 | 1.11 | 7.8125E-03 | 1.00 |

**Table 3.** Results for $k = l + 1 = m + 1 = 2$ with $t = 1$: Ladder-shaped meshes

| Mesh | $\frac{\|\boldsymbol{\theta}-\boldsymbol{\theta}_h\|_{\mathcal{T}_h}}{\|\boldsymbol{\theta}\|_0}$ | | $\frac{\|\nabla\boldsymbol{\theta}-\nabla\boldsymbol{\theta}_h\|_{\mathcal{T}_h}}{\|\nabla\boldsymbol{\theta}\|_0}$ | | $\frac{\|\boldsymbol{\sigma}-\boldsymbol{\sigma}_h\|_{\mathcal{T}_h}}{\|\boldsymbol{\sigma}\|_0}$ | |
|---|---|---|---|---|---|---|
| | Error | Rate | Error | Rate | Error | Rate |
| $4 \times 4$ | 7.7832E-02 | | 3.1407E-01 | | 2.8919E-01 | |
| $8 \times 8$ | 1.1931E-02 | 2.71 | 9.7364E-02 | 1.69 | 8.7805E-02 | 1.72 |
| $16 \times 16$ | 1.8504E-03 | 2.69 | 2.7373E-02 | 1.83 | 2.3720E-02 | 1.89 |
| $32 \times 32$ | 2.6185E-04 | 2.82 | 7.2957E-03 | 1.91 | 6.1291E-03 | 1.95 |
| $64 \times 64$ | 3.4723E-05 | 2.91 | 1.8826E-03 | 1.95 | 1.5552E-03 | 1.98 |
| $128 \times 128$ | 4.4622E-06 | 2.96 | 4.7791E-04 | 1.98 | 3.9150E-04 | 1.99 |
| Mesh | $\frac{\|w-w_h\|_{\mathcal{T}_h}}{\|w\|_0}$ | | $\frac{\|\nabla w-\nabla w_h\|_{\mathcal{T}_h}}{\|\nabla w\|_0}$ | | $\frac{(t+h^2)\|\gamma-\gamma_h\|_{\mathcal{T}_h}}{\|\gamma\|_0}$ | |
| | Error | Rate | Error | Rate | Error | Rate |
| $4 \times 4$ | 9.6871E-02 | | 4.6849E-01 | | 1.4047E-01 | |
| $8 \times 8$ | 1.3449E-02 | 2.85 | 1.3844E-01 | 1.76 | 2.8855E-02 | 2.28 |
| $16 \times 16$ | 1.6913E-03 | 2.99 | 3.6252E-02 | 1.93 | 6.5449E-03 | 2.14 |
| $32 \times 32$ | 2.0993E-04 | 3.01 | 9.1628E-03 | 1.98 | 1.5889E-03 | 2.04 |
| $64 \times 64$ | 2.6105E-05 | 3.01 | 2.2977E-03 | 2.00 | 3.9380E-04 | 2.01 |
| $128 \times 128$ | 3.2534E-06 | 3.00 | 5.7499E-04 | 2.00 | 9.8155E-05 | 2.00 |

**Table 4.** Results for $k = l + 1 = m + 1 = 2$ with $t = 10^{-10}$: Ladder-shaped meshes

| Mesh | $\frac{\|\boldsymbol{\theta}-\boldsymbol{\theta}_h\|_{\mathcal{T}_h}}{\|\boldsymbol{\theta}\|_0}$ | | $\frac{\|\nabla\boldsymbol{\theta}-\nabla\boldsymbol{\theta}_h\|_{\mathcal{T}_h}}{\|\nabla\boldsymbol{\theta}\|_0}$ | | $\frac{\|\boldsymbol{\sigma}-\boldsymbol{\sigma}_h\|_{\mathcal{T}_h}}{\|\boldsymbol{\sigma}\|_0}$ | |
|---|---|---|---|---|---|---|
| | Error | Rate | Error | Rate | Error | Rate |
| $4 \times 4$ | 6.5594E-02 | | 3.1506E-01 | | 2.8704E-01 | |
| $8 \times 8$ | 1.0066E-02 | 2.70 | 9.6546E-02 | 1.71 | 8.7164E-02 | 1.72 |
| $16 \times 16$ | 1.4578E-03 | 2.79 | 2.6454E-02 | 1.87 | 2.3500E-02 | 1.89 |
| $32 \times 32$ | 2.1777E-04 | 2.74 | 7.0561E-03 | 1.91 | 6.0716E-03 | 1.95 |
| $64 \times 64$ | 3.1158E-05 | 2.81 | 1.8443E-03 | 1.94 | 1.5425E-03 | 1.98 |
| $128 \times 128$ | 4.1709E-06 | 2.90 | 4.7227E-04 | 1.97 | 3.8864E-04 | 1.99 |
| Mesh | $\frac{\|w-w_h\|_{\mathcal{T}_h}}{\|w\|_0}$ | | $\frac{\|\nabla w-\nabla w_h\|_{\mathcal{T}_h}}{\|\nabla w\|_0}$ | | $\frac{(t+h^2)\|\gamma-\gamma_h\|_{\mathcal{T}_h}}{\|\gamma\|_0}$ | |
| | Error | Rate | Error | Rate | Error | Rate |
| $4 \times 4$ | 5.3199E-01 | | 3.0600E+00 | | 6.2500E-02 | |
| $8 \times 8$ | 3.7876E-02 | 3.81 | 4.8988E-01 | 2.64 | 1.5625E-02 | 2.00 |
| $16 \times 16$ | 2.5500E-03 | 3.89 | 6.7529E-02 | 2.86 | 3.9063E-03 | 2.00 |
| $32 \times 32$ | 1.7372E-04 | 3.88 | 9.9753E-03 | 2.76 | 9.7656E-04 | 2.00 |
| $64 \times 64$ | 1.3356E-05 | 3.70 | 1.7924E-03 | 2.48 | 2.4414E-04 | 2.00 |
| $128 \times 128$ | 1.2819E-06 | 3.38 | 3.9266E-04 | 2.19 | 6.1035E-05 | 2.00 |

**Table 5.** Results for $k = l + 1 = m + 1 = 3$ with $t = 1$: Nonconforming meshes

| Mesh | $\frac{\|\boldsymbol{\theta}-\boldsymbol{\theta}_h\|_{\mathcal{T}_h}}{\|\boldsymbol{\theta}\|_0}$ | | $\frac{\|\nabla\boldsymbol{\theta}-\nabla\boldsymbol{\theta}_h\|_{\mathcal{T}_h}}{\|\nabla\boldsymbol{\theta}\|_0}$ | | $\frac{\|\boldsymbol{\sigma}-\boldsymbol{\sigma}_h\|_{\mathcal{T}_h}}{\|\boldsymbol{\sigma}\|_0}$ | |
|---|---|---|---|---|---|---|
| | Error | Rate | Error | Rate | Error | Rate |
| $4 \times 4$ | 3.5007E-02 | | 1.4850E-01 | | 1.2049E-01 | |
| $8 \times 8$ | 1.6536E-03 | 4.40 | 1.7657E-02 | 3.07 | 1.5091E-02 | 3.00 |
| $16 \times 16$ | 9.5059E-05 | 4.12 | 2.1713E-03 | 3.02 | 1.9100E-03 | 2.98 |
| $32 \times 32$ | 5.2505E-06 | 4.18 | 2.5643E-04 | 3.08 | 2.2745E-04 | 3.07 |
| $64 \times 64$ | 2.9668E-07 | 4.15 | 3.0472E-05 | 3.07 | 2.7106E-05 | 3.07 |
| Mesh | $\frac{\|w-w_h\|_{\mathcal{T}_h}}{\|w\|_0}$ | | $\frac{\|\nabla w-\nabla w_h\|_{\mathcal{T}_h}}{\|\nabla w\|_0}$ | | $\frac{(t+h^3)\|\gamma-\gamma_h\|_{\mathcal{T}_h}}{\|\gamma\|_0}$ | |
| | Error | Rate | Error | Rate | Error | Rate |
| $4 \times 4$ | 3.6904E-02 | | 1.8311E-01 | | 6.9324E-02 | |
| $8 \times 8$ | 2.9256E-03 | 3.66 | 2.9497E-02 | 2.63 | 6.4868E-03 | 3.42 |
| $16 \times 16$ | 1.5034E-04 | 4.28 | 3.2052E-03 | 3.20 | 7.0521E-04 | 3.20 |
| $32 \times 32$ | 7.9527E-06 | 4.24 | 3.5503E-04 | 3.17 | 7.6865E-05 | 3.20 |
| $64 \times 64$ | 4.3067E-07 | 4.21 | 4.0630E-05 | 3.13 | 8.7066E-06 | 3.14 |

**Table 6.** Results for $k = l + 1 = m + 1 = 3$ with $t = 10^{-10}$: Nonconforming meshes

| Mesh | $\frac{\|\boldsymbol{\theta}-\boldsymbol{\theta}_h\|_{\mathcal{T}_h}}{\|\boldsymbol{\theta}\|_0}$ | | $\frac{\|\nabla\boldsymbol{\theta}-\nabla\boldsymbol{\theta}_h\|_{\mathcal{T}_h}}{\|\nabla\boldsymbol{\theta}\|_0}$ | | $\frac{\|\boldsymbol{\sigma}-\boldsymbol{\sigma}_h\|_{\mathcal{T}_h}}{\|\boldsymbol{\sigma}\|_0}$ | |
|---|---|---|---|---|---|---|
| | Error | Rate | Error | Rate | Error | Rate |
| $4 \times 4$ | 2.8790E-02 | | 1.4409E-01 | | 1.1992E-01 | |
| $8 \times 8$ | 1.4758E-03 | 4.29 | 1.7400E-02 | 3.05 | 1.5056E-02 | 2.99 |
| $16 \times 16$ | 8.7510E-05 | 4.08 | 2.1514E-03 | 3.02 | 1.9066E-03 | 2.98 |
| $32 \times 32$ | 5.0320E-06 | 4.12 | 2.5565E-04 | 3.07 | 2.2729E-04 | 3.07 |
| $64 \times 64$ | 2.9100E-07 | 4.11 | 3.0455E-05 | 3.07 | 2.7102E-05 | 3.07 |
| Mesh | $\frac{\|w-w_h\|_{\mathcal{T}_h}}{\|w\|_0}$ | | $\frac{\|\nabla w-\nabla w_h\|_{\mathcal{T}_h}}{\|\nabla w\|_0}$ | | $\frac{(t+h^3)\|\boldsymbol{\gamma}-\boldsymbol{\gamma}_h\|_{\mathcal{T}_h}}{\|\boldsymbol{\gamma}\|_0}$ | |
| | Error | Rate | Error | Rate | Error | Rate |
| $4 \times 4$ | 2.7780E-01 | | 1.9311E+00 | | 1.5625E-02 | |
| $8 \times 8$ | 7.4371E-03 | 5.22 | 1.1006E-01 | 4.13 | 1.9531E-03 | 3.00 |
| $16 \times 16$ | 2.8842E-04 | 4.69 | 8.0965E-03 | 3.76 | 2.4414E-04 | 3.00 |
| $32 \times 32$ | 8.6548E-06 | 5.06 | 5.1452E-04 | 3.98 | 3.0518E-05 | 3.00 |
| $64 \times 64$ | 2.5255E-07 | 5.10 | 3.6934E-05 | 3.80 | 3.8148E-06 | 3.00 |

## 5.2. *Square Plate II*

In this example, the domain is set as $\Omega = (0, L)^2$ with $L = 10$, and the material parameters are taken as $E = 10920, \nu = 0.3, \kappa = \frac{5}{6}, \boldsymbol{f} = \boldsymbol{0}, g = 1$. Both the hard clamped (HC) and soft simply supported (SSS) boundary conditions are considered. The meshes are as same as in Figs. 1-3. The results in Table 7, where $w_c$ and $M_c$ are respectively the displacement $w_h$ and the moment $\max_{i,j} |(\boldsymbol{\sigma}_h)_{i,j}|$ at the center of the plate on the $192 \times 192$ mesh, show that the HDG method with $k = l = m = 1$ is of uniformly good accuracy.

**Table 7.** Results for Square Plate II on $192 \times 192$ mesh ($k = l = m = 1$)

| | $t$ | $10^{-1}$ | $10^{-4}$ | $10^{-6}$ | $10^{-9}$ | $10^{-14}$ | Reference |
|---|---|---|---|---|---|---|---|
| HC condition | $w_c/(10^{-5}gL^4/D)$ | 126.8 | 126.5 | 126.5 | 126.5 | 126.5 | 126.5 |
| Triangle mesh | $M_c/(10^{-4}gL^2/D)$ | 229.1 | 229.1 | 229.1 | 229.1 | 229.1 | 231.0 |
| HC condition | $w_c/(10^{-5}gL^4/D)$ | 126.8 | 126.5 | 126.5 | 126.5 | 126.5 | 126.5 |
| Ladder-shaped mesh | $M_c/(10^{-4}gL^2/D)$ | 229.1 | 229.1 | 229.1 | 229.1 | 229.1 | 231.0 |
| HC condition | $w_c/(10^{-5}gL^4/D)$ | 126.8 | 126.5 | 126.5 | 126.5 | 126.5 | 126.5 |
| Nonconforming mesh | $M_c/(10^{-4}gL^2/D)$ | 229.1 | 229.1 | 229.1 | 229.1 | 229.1 | 231.0 |
| SSS condition | $w_c/(10^{-5}gL^4/D)$ | 410.0 | 407.1 | 407.1 | 407.1 | 407.1 | 406.2* |
| Triangle mesh | $M_c/(10^{-4}gL^2/D)$ | 482.1 | 479.6 | 479.6 | 479.6 | 479.6 | 479.0 |
| SSS condition | $w_c/(10^{-5}gL^4/D)$ | 410.2 | 407.6 | 407.6 | 407.6 | 407.6 | 406.2* |
| Ladder-shaped mesh | $M_c/(10^{-4}gL^2/D)$ | 482.3 | 480.2 | 480.2 | 480.2 | 480.2 | 479.0 |
| SSS condition | $w_c/(10^{-5}gL^4/D)$ | 410.2 | 407.4 | 407.4 | 407.4 | 407.4 | 406.2* |
| Nonconforming mesh | $M_c/(10^{-4}gL^2/D)$ | 482.1 | 479.9 | 479.9 | 479.9 | 479.9 | 479.0 |

* 406.4 for $t = 10^{-1}$.

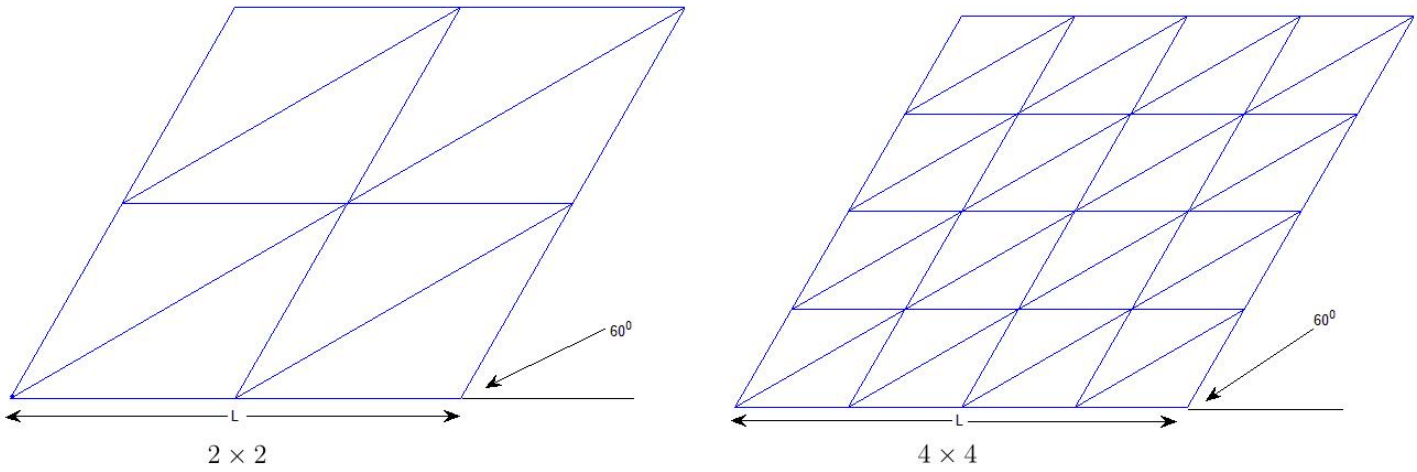


**Fig. 4.** Triangle meshes for Razzaque's skew plate

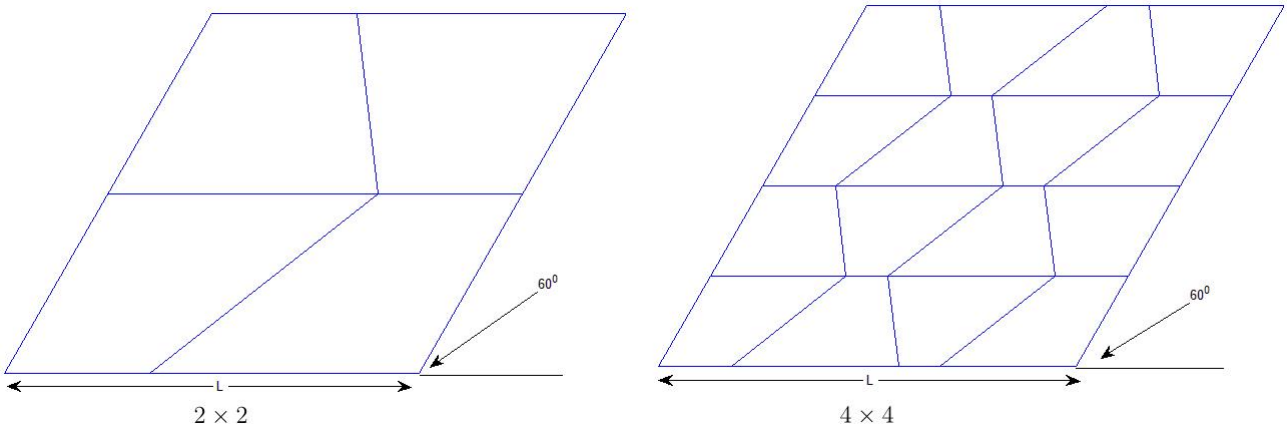


**Fig. 5.** Quadrangle meshes for Razzaque's skew plate

### 5.3. *Razzaque's skew plate* (60°)

The domain and computational meshes in Figs. 4-5 are simply obtained by multiplying the mesh coordinates in Figs. 1-2 by the matrix

$$A = 100 \begin{pmatrix} 1 & \frac{1}{2} \\ 0 & \frac{\sqrt{3}}{2} \end{pmatrix}.$$

The material parameters are taken as $E = 1280, \kappa = \frac{5}{6}, \nu = 0.3, L = 100, \boldsymbol{f} = \mathbf{0}, g = 1$ and $t = 0.1$. The plate is simply supported on the upper-side and under-side and free on the other two sides. The results in Table 8, where the central principal moments $M_c^1 = (\boldsymbol{\sigma}_h)_{11}$ and $M_c^2 = (\boldsymbol{\sigma}_h)_{22}$, show that the HDG method with $k = l = m = 1$ is of good accuracy.

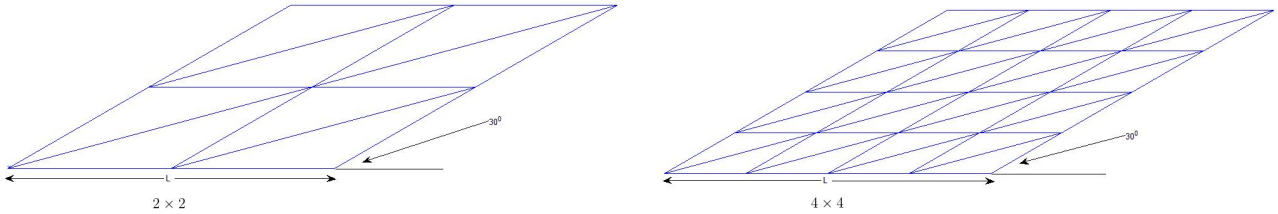


**Fig. 6.** Triangle meshes for Morley's simply supported rhombic plate

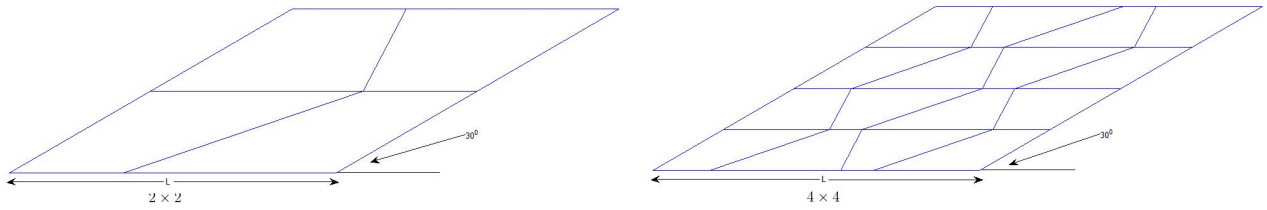


**Fig. 7.** Quadrangle meshes for Morley's simply supported rhombic plate

**Table 8.** Results for Razzaque's skew plate (60°) ($k = l = m = 1$)

| | Mesh | $32 \times 32$ | $64 \times 64$ | $128 \times 128$ | $192 \times 192$ | Reference* |
|---|---|---|---|---|---|---|
| Triangle Mesh | $w_c/(10^{-3}L^4/D)$ | 7.998748 | 7.951844 | 7.930071 | 7.923238 | 7.945 |
| | $-M_c^1/(10^{-2}gL^2)$ | 1.406363 | 1.501475 | 1.542217 | 1.554424 | |
| | $-M_c^2/(10^{-2}gL^2)$ | 9.653932 | 9.627260 | 9.613297 | 9.608788 | 9.589 |
| Qarangle Mesh | $w_c/(10^{-3}L^4/D)$ | 8.066981 | 7.986796 | 7.946969 | 7.934098 | 7.945 |
| | $-M_c^1/(10^{-2}gL^2)$ | 1.284099 | 1.445068 | 1.517459 | 1.539256 | |
| | $-M_c^2/(10^{-2}gL^2)$ | 9.703351 | 9.650286 | 9.624435 | 9.616006 | 9.589 |

* Finite difference solution on $16 \times 16$ mesh.[50]

**Table 9.** Results for Morley's soft simply supported rhombic plate ($30°$) ($k = l = m = 1$)

| | Mesh | $t = 1$ | | | $t = 0.01$ | | |
|---|---|---|---|---|---|---|---|
| | | $\frac{w_c}{10^{-3}gL^4/D}$ | $-\frac{M_c^1}{10^{-2}gL^2}$ | $-\frac{M_c^2}{10^{-2}gL^2}$ | $\frac{w_c}{10^{-3}gL^4/D}$ | $-\frac{M_c^1}{10^{-2}gL^2}$ | $-\frac{M_c^2}{10^{-2}gL^2}$ |
| SSS condition Triangle mesh | $32 \times 32$ | 0.436418 | 1.243484 | 1.947566 | 0.435064 | 1.241963 | 1.944920 |
| | $64 \times 64$ | 0.430739 | 1.220826 | 1.920798 | 0.428567 | 1.216877 | 1.915387 |
| | $128 \times 128$ | 0.427308 | 1.207124 | 1.908869 | 0.423628 | 1.198215 | 1.898636 |
| | $192 \times 192$ | 0.426164 | 1.202756 | 1.905353 | 0.421298 | 1.189744 | 1.891450 |
| | Reference | 0.408* | 1.08 | 1.91 | 0.419** | | |
| SSS condition Quadrangle mesh | $32 \times 32$ | 0.438826 | 1.238748 | 1.944255 | 0.437723 | 1.237821 | 1.942615 |
| | $64 \times 64$ | 0.430380 | 1.221711 | 1.923048 | 0.430314 | 1.218984 | 1.919273 |
| | $128 \times 128$ | 0.427837 | 1.208232 | 1.910332 | 0.424865 | 1.201452 | 1.902543 |
| | $192 \times 192$ | 0.426396 | 1.203286 | 1.906013 | 0.422338 | 1.192829 | 1.894809 |
| | Reference | 0.408* | 1.08 | 1.91 | 0.419** | | |

* A three-dimensional solution by Babuška and Scapolla[6] is 0.423.
** Two-dimensional solution by Carstensen, Xie, Yu and Zho.u[?]

### *5.4. Morley's simply supported rhombic plate ($30°$)*

This test is a very critical one. The domain and computational meshes in Figs. 6-7 are simply obtained by multiplying the meshes in Figs. 1-2 by the matrix

$$A = 100 \begin{pmatrix} 1 & \frac{\sqrt{3}}{2} \\ 0 & \frac{1}{2} \end{pmatrix}.$$

The material parameters are taken as $E = 1000, \kappa = \frac{5}{6}, \nu = 0.3, L = 100, \boldsymbol{f} = \mathbf{0}, g = 1$. The soft simply supported boundary condition is used. The results in Table 9 show that the HDG method with $k = l = m = 1$ is of good accuracy.

## 6. Conclusion

In this paper we have developed an arbitrary order shear-locking-free HDG method for numerical analysis of the Reissner-Mindlin plates. Optimal error estimates which are uniform in the plate thickness have been derived, and numerical experiments have confirmed the theoretical analysis.

## Acknowledgments

This work was partially supported by National Natural Science Foundation of China (11801063, 11771312), the Fundamental Research Funds for the Central Universities (YJ202030), and China Postdoctoral Science Foundation (2018M633339, 2019T120828)

## Conflicts of Interest

The authors declare no conflict of interest.

## References

1 Arnold D.N. Discretization by Finite Elements of a Model Parameter dependent problem. *Numer. Math.*, 1981, **37**, 405-421. [CrossRef]
2 Arnold D.N. An interior penalty finite element method with discontinuous elements. *SIAM J. Numer. Anal.*, 1982, **19**, 742-760. [CrossRef]
3 Arnold D.N.; Brezzi F.; Cockburn B.; Marini L.D. Unified analysis of discontinuous Galerkin methods for elliptic problems. *SIAM J. Numer. Anal.*, 2002, **39**, 1749-1779. [CrossRef]
4 Arnold D.N.; Falk R.S. A uniformly accurate finite element method for the Reissner-Mindlin plate. *SIAM J. Numer. Anal.*, 1989, **26**, 1276-1290. [CrossRef]
5 Ayad R.; Dhatt G.; Batoz J.L. A new hybrid-mixed variational approach for Reissner–Mindlin plates. The MiSP model. *Int. J. Numer. Methods Eng.*, 1998, **42**, 1149-1179. [CrossRef]
6 Babuška I.; Scapolla T. Benchmark computation and performance evaluation for a rhombic plate bending problem. *Int. J. Numer. Methods Eng.*., 1989, **28**, 155-179. [CrossRef]
7 Boffi D.; Brezzi F.; Fortin M. Mixed finite element methods and applications. Vol. 44 of Springer Series in Computational Mathematics, Springer, Heidelberg, 2013. [Link]

8 Braess D. Finite elements. Cambridge University Press, Cambridge, second ed., 2001. Theory, fast solvers, and applications in solid mechanics, Translated from the 1992 German edition by Larry L. Schumaker. [Link]
9 Brenner S.C. Poincaré-Friedrichs inequalities for piecewise $H^1$ functions. *SIAM J. Numer. Anal.*, 2003, **41**, 306-324. [CrossRef]
10 Brenner S.C. Korn's inequalities for piecewise $H^1$ vector fields. *Math. Comp.*, 2004, **73**, 1067-1087. [CrossRef]
11 Brezzi F.; Fortin M. Numerical approximation of Mindlin-Reissner plates. *Math. Comput.*, 1986, **47**, 151-158. [CrossRef]
12 Brezzi F.; Fortin M. Mixed and hybrid finite element methods, Vol. 15 of Springer Series in Computational Mathematics. *Springer-Verlag*, New York, 1991. [CrossRef]
13 Brezzi F.; Fortin M.; Stenberg R. Error analysis of mixed-interpolated elements for Reissner-Mindlin plates. *Math. Models Methods Appl. Sci.*, 1991, **1**, 125-151. [CrossRef]
14 Carrero J.; Cockburn B.; Schötzau D. Hybridized globally divergence-free LDG methods. I. The Stokes problem. *Math. Comp.*, 2006, **75**, 533-563. [CrossRef]
15 Carstensen C.; Xie X.; Yu G.; Zhou T. A priori and a posteriori analysis for a locking-free low order quadrilateral hybrid finite element for reissner-mindlin plates. *Comput. Methods Appl. Mech. Eng.*, 2011, **200**, 1161-1175. [CrossRef]
16 Castillo P.; Cockburn B.; Perugia I.; Schötzau D. An a priori error analysis of the local discontinuous Galerkin method for elliptic problems. *SIAM J. Numer. Anal.*, 2000, **38**, 1676-1706. [CrossRef]
17 Cesmelioglu A.; Cockburn B.; Nguyen N.C.; Peraire J. Analysis of HDG methods for Oseen equations. *J. Sci. Comput.*, 2013, **55**, 392-431. [CrossRef]
18 Chen H.; Qiu W.; Shi K.; Solano M. A superconvergent HDG method for the Maxwell equations. *J. Sci. Comput.*, 2017, **70**, 1010-1029. [CrossRef]
19 Cockburn B.; Cui J. An analysis of HDG methods for the vorticity-velocity-pressure formulation of the Stokes problem in three dimensions. *Math. Comp.*, 2012, **81**, 1355-1368. [CrossRef]
20 Cockburn B.; Gopalakrishnan J. Incompressible finite elements via hybridization. I. The Stokes system in two space dimensions. *SIAM J. Numer. Anal.*, 2005, **43**, 1627-1650. [CrossRef]
21 Cockburn B.; Gopalakrishnan J. Incompressible finite elements via hybridization. II. The Stokes system in three space dimensions. *SIAM J. Numer. Anal.*, 2005, **43**, 1651-1672. [CrossRef]
22 Cockburn B.; Gopalakrishnan J. The derivation of hybridizable discontinuous Galerkin methods for Stokes flow. *SIAM J. Numer. Anal.*, 2009, **47**, 1092-1125. [CrossRef]
23 Cockburn B.; Gopalakrishnan J.; Lazarov R. Unified hybridization of discontinuous Galerkin, mixed, and continuous Galerkin methods for second order elliptic problems. *SIAM J. Numer. Anal.*, 2009, **47**, 1319-1365. [CrossRef]
24 Cockburn B.; Gopalakrishnan J.; Sayas F.-J. A projection-based error analysis of HDG methods. *Math. Comp.*, 2010, **79**, 1351-1367. [CrossRef]
25 Cockburn B.; Kanschat G.; Schötzau D. A locally conservative LDG method for the incompressible Navier-Stokes equations. *Math. Comp.*, 2005, **74**, 1067-1095. [CrossRef]
26 Cockburn B.; Shi K. Conditions for superconvergence of HDG methods for Stokes flow. *Math. Comp.*, 2013, **82**, 651-671. [CrossRef]
27 Cockburn B.; Shi K. Devising **HDG** methods for Stokes flow: an overview. *Comput. & Fluids*, 2014, **98**, 221-229. [CrossRef]
28 Cockburn B.; Shu C.-W. The local discontinuous Galerkin method for time-dependent convection-diffusion systems. *SIAM J. Numer. Anal.*, 1998, **35**, 2440-2463. [CrossRef]
29 Demkowicz L. Gopalakrishnan J. Analysis of the DPG method for the Poisson equation. *SIAM J. Numer. Anal.*, 2011, **49**, 1788-1809. [CrossRef]
30 Durán R.; Liberman E. On mixed finite element methods for the Reissner-Mindlin plate model. *Math. Comp.*, 1992, **58**, 561-573. [CrossRef]
31 Falk R.S.; Tu T. Locking-free finite elements for the Reissner-Mindlin plate. *Math. Comp.*, 2000, **69**, 911-928. [CrossRef]
32 Gaël Guennebaud B.J. et al. Eigen 3.2.7. 2015. [Link]
33 Guo Y.; Yu G.; Xie X. Uniform analysis of a stabilized hybrid finite element method for ressiner-mindlin plates. *Sci. China Math.*, 2013, **56**, 1727-1742. [CrossRef]
34 Hu J.; Ming P.; Shi Z. Nonconforming quadrilateral rotated $Q_1$ element for Reissner-Mindlin plate.*J. Comput. Math.*, 2003, **21** 25-32. Special issue dedicated to the 80th birthday of Professor Zhou Yulin. [CrossRef]
35 Hu J.; Shi Z.-C. Two lower order nonconforming rectangular elements for the Reissner-Mindlin plate. *Math. Comp.*, **76**, 1771-1786. [CrossRef]
36 Hu J.; Shi Z.-C. Error analysis of quadrilateral Wilson element for Reissner-Mindlin plate. *Comput. Methods Appl. Mech. Eng.*, 2008, **197**, 464-475. [CrossRef]
37 Hu J.; Shi Z.-C. Analysis for quadrilateral MITC elements for the Reissner-Mindlin plate problem. *Math. Comp.*, 2009, **78**, 673-711. [CrossRef]
38 Li B.; Xie X. Analysis of a family of HDG methods for second order elliptic problems. *J. Comput. Appl. Math.*, 2016, **307**, 37-51. [CrossRef]
39 Li B.; Xie X.; Zhang S. Analysis of a two-level algorithm for HDG methods for diffusion problems. *Commun. Comput. Phys.*, 2015, **19**, 1435-1460. [CrossRef]
40 Lovadina C. A low-order nonconforming finite element for Reissner-Mindlin plates. *SIAM J. Numer. Anal.*, 2005, **42**, 2688-2705. [CrossRef]
41 Amara M.; Capatina-Papaghiuc, D.; Chatti A. New locking-free mixed method for the reissner-mindlin thin plate model. *SIAM J. Numer. Anal.*, 2003, **40**, 1561-1582. [CrossRef]
42 Ming P.; Shi Z.-C. Nonconforming rotated $q^1$ element for Reissner-Mindlin plate. *Math. Models Methods Appl. Sci.*, 2001, **11**, 1311-1342. [CrossRef]
43 Ming P.; Shi Z.C. Two nonconforming quadrilateral elements for the Reissner-Mindlin plate. *Math. Models Methods Appl. Sci.*, 2005,

**15**, 1503-1517. [CrossRef]
44 Ming P.; Shi Z.C. Analysis of some low order quadrilateral Reissner-Mindlin plate elements. *Math. Comp*., 2006, **75**, 1043-1065. [CrossRef]
45 Nguyen N.C.; Peraire J.; Cockburn B. A hybridizable discontinuous Galerkin method for Stokes flow. *Comput. Methods Appl. Mech. Eng*., 2010, **199**, 582-597. [CrossRef]
46 Pitkäranta J.; Suri M. Design principles and error analysis for reduced-shear plate-bending finite elements. *Numer. Math*., 1996, **75**, 223-266. [CrossRef]
47 Qiu W.; Shen J.; Shi K. An HDG method for linear elasticity with strong symmetric stresses. *Math. Comp*., 2018, **87**, 69-93. [CrossRef]
48 Qiu W.; Shi K. An HDG method for convection diffusion equation. *J. Sci. Comput*., 2016, **66**, 346-357. [CrossRef]
49 Qiu W.; Shi K. A superconvergent HDG method for the incompressible Navier-Stokes equations on general polyhedral meshes. *IMA J. Numer. Anal*., 2016, **36**, 1943-1967. [CrossRef]
50 Razzaque A. Program for triangular bending elements with derivative smoothing. *Int. J. Numer. Methods Eng*., 1973, **6**, 333-343. [CrossRef]
51 Yu G.; Xie X. Analysis of 3-node mixed-shear-projected triangular element method for reissner-mindlin plates. *Numer. Meth. PDEs*, 2017, **33**, 241-258. [CrossRef]
52 Yu G.; Xie X.; Guo Y. Analysis of mixed-shear-projected quadrilateral element method for reissner-mindlin plates. *Int. J. Numer. Anal. Mod*., 2017, **14**, 48-62. [CrossRef]
53 Zhang Z.; Zhang S. Wilson's element for the Reissner-Mindlin plate. *Comput. Methods Appl. Mech. Eng*., 1994, **113**, 55-65. [CrossRef]